1988-09

Processing of Aluminum alloy 2090 for superplasticity

Groh, Gary E.

NAVAL POSTGRADUATE SCHOOL
Monterey, California

THESIS

PROCESSING OF ALUMINUM ALLOY
2090 FOR SUPERPLASTICITY

BY

Gary E. Groh

September 1988

Thesis Co-Advisors: T. R. McNelley
S. J. Hales

Approved for public release; distribution is unlimited.

UNCLASSIFIED
SECURITY CLASSIFICATION OF THIS PAGE

REPORT DOCUMENTATION PAGE

1a REPORT SECURITY CLASSIFICATION UNCLASSIFIED	1b RESTRICTIVE MARKINGS
2a SECURITY CLASSIFICATION AUTHORITY	3 DISTRIBUTION/AVAILABILITY OF REPORT Approved for public release, distribution is unlimitted.
2b DECLASSIFICATION/DOWNGRADING SCHEDULE	
4 PERFORMING ORGANIZATION REPORT NUMBER(S)	5 MONITORING ORGANIZATION REPORT NUMBER(S)
6a NAME OF PERFORMING ORGANIZATION Naval Postgraduate School 6b OFFICE SYMBOL (If applicable) Code 69	7a NAME OF MONITORING ORGANIZATION
6c. ADDRESS (City, State, and ZIP Code) Monterey, California 93943-5000	7b. ADDRESS (City, State, and ZIP Code) Monterey, California 93943-5000
8a. NAME OF FUNDING/SPONSORING ORGANIZATION 8b OFFICE SYMBOL (If applicable)	9 PROCUREMENT INSTRUMENT IDENTIFICATION NUMBER
8c. ADDRESS (City, State, and ZIP Code)	10 SOURCE OF FUNDING NUMBERS PROGRAM ELEMENT NO / PROJECT NO. / TASK NO / WORK UNIT ACCESSION NO

11. TITLE (Include Security Classification)

Processing of Aluminum Alloy 2090 for Superplasticity

12 PERSONAL AUTHOR(S)

13a TYPE OF REPORT	13b TIME COVERED	14 DATE OF REPORT (Year, Month, Day)	15 PAGE COUNT
Master's Thesis	FROM _____ TO _____	1988, September	83

16 SUPPLEMENTARY NOTATION
The views expressed in this thesis are those of the author and do not reflect the official policy or position of the Department of Defense or U.S Govt.

17 COSATI CODES			18 SUBJECT TERMS (Continue on reverse if necessary and identify by block number)
FIELD	GROUP	SUB-GROUP	Aluminum-Copper-Lithium Alloys 2090, Thermomechanically Processing, Superplasticity

19 ABSTRACT (Continue on reverse if necessary and identify by block number)

Existing superplastic forming techniques for Al alloys rely on deformation at temperatures of 500°C to achieve the desired ductilities. The Al alloy 2090 (Al-Li-Cu-Zr) has been successfully fabricated by such techniques, but at temperatures where cavitation during formation may significantly reduce the mechanical properties of the final product. It has been previously shown that cavitation can be effectively supressed by forming at lower temperatures. The purpose of this research is to investigate the applicability of thermomechanical processing methods (developed at NPS for Al-Mg-X alloys) to produce a refined microstructure capable of supporting superplasticity at lower temperatures in Al 2090.

20 DISTRIBUTION/AVAILABILITY OF ABSTRACT ☒ UNCLASSIFIED/UNLIMITED ☐ SAME AS RPT ☐ DTIC USERS	21 ABSTRACT SECURITY CLASSIFICATION UNCLASSIFIED
22a NAME OF RESPONSIBLE INDIVIDUAL Professor T. R. McNelley	22b TELEPHONE (Include Area Code) (408) 646-2589 22c OFFICE SYMBOL 69Mc

DD FORM 1473, 84 MAR 83 APR edition may be used until exhausted
All other editions are obsolete

SECURITY CLASSIFICATION OF THIS PAGE

☆ U.S. Government Printing Office: 1986—606-24

Approved for public release; distribution unlimited.

Processing of Aluminum Alloy 2090 for Superplasticity

by

Gary E. Groh
Lieutenant Commander, United States Navy
B.S.M.E. United States Naval Academy, 1974

Submitted in partial fulfillment of the
requirements for the degree of

MASTER OF SCIENCE IN MECHANICAL ENGINEERING

ABSTRACT

Existing superplastic forming techniques for Al alloys rely on deformation at temperatures of 500°C to achieve the desired ductilities. The Al alloy 2090 (Al-Li-Cu-Zr) has been successfully fabricated by such techniques, but at temperatures where cavitation during forming may significantly reduce the mechanical properties of the final product. It has been previously shown that cavitation can be effectively suppressed by forming at lower temperatures. The purpose of this research is to investigate the applicability of thermomechanical processing methods (developed at NPS for Al-Mg-X alloys) to produce a refined microstructure capable of supporting superplasticity at lower temperatures in Al 2090.

TABLE OF CONTENTS

ACKNOWLEDGEMENT

I would like to express my sincere thanks to my advisor, Professor T. R. McNelley, and my co-advisor, Dr. S. J. Hales for their guidance and tireless assistance in conducting this study. The technical assistance of Mr. T. Kellogg in conducting the experimental work, and Mr. R. Hafley in preparing the diagrams for this work, is also appreciated. I would also like to acknowledge the Aluminum Company of America (ALCOA) for providing the sample material, and Naval Air Systems Command for sponsoring this research.

LIST OF FIGURES

I. INTRODUCTION

Many Al alloys with moderate to high solute contents become highly susceptible to intergranular attack by corrosion because of extensive grain boundary precipitation [Ref 1,2]. The initial intent of work on the Al-10Mg-0.1Zr alloy in this laboratory was to implement an intermediate temperature (300°C) processing scheme to induce precipitation of the intermetallic β phase (Al_8Mg_5) concurrently with deformation by rolling [Ref. 3]. The net result was a uniform distribution of the β phase as discrete particles (0.5-1.0μm) throughout the microstructure and consequently a reduction in the number of coarse intergranular precipitates.

The microstructure attained was also shown to be superplastic at 300°C and subsequent studies were aimed at optimizing this response [Ref. 4]. It was determined that a high dislocation density, induced by large rolling strains and large reductions per rolling pass, in conjunction with sufficient static annealing time between rolling passes, produced the highest ductilities [Ref. 5]. Further investigations indicated that fine-grains 2-5μm in size evolved by continuous recrystallization during the TMP itself [Ref. 6].

The decoration of grain boundaries by second phase precipitates has proved to be very detrimental to mechanical

properties in Al 2090 [Ref. 7]. Attempts to counteract this have focussed on stretching at ambient temperatures prior to aging treatments designed to improve strength [Ref. 8]. The stretching introduces dislocations into the matrix thereby increasing the number of potential nucleation sites for precipitation of second phases. The net result is an increase in the amount of intragranular precipitation and a decrease in the size and spacing of the intergranular precipitates. This modification has proved very effective in producing the desired mechanical properties in the final product [Ref. 9]. However, with the advent of near net shape forming, in particular superplastic forming, subsequent stretching of complex shapes is impractical. Forming operations are usually conducted at temperatures in excess of 500°C such that aging treatments are required to obtain optimum mechanical properties in the final product. In addition, Al 2090 is prone to cavitation at the forming temperatures currently employed and the strength levels achieved are far below those desired [Ref. 10].

The intent of this research is to apply to alloy 2090 lower temperature (300°C) thermomechanical processing techniques developed over the last several years at the Naval Postgraduate School for the Al-Mg-X alloys [Ref. 3,4]. With 2090 the processing involves solution treatment at 540°C, hot working at 480°C, followed by 10% cold work, aging at 350°C, and warm rolling to a true strain of 2.5, while keeping the

reduction per pass constant at 10%, and maintaining isothermal conditions by reheating the material between the rolling passes. During processing of the Al-Mg alloys, the β phase has been determined to play a vital role in the development of a superplastic microstructure [Ref. 5]. In order to obtain a similar precipitate distribution in the Al 2090 alloy, it is anticipated that the T_2 precipitates would have to be present at the onset of warm rolling. Thus, in an attempt to produce a continuously recrystallized grain structure during processing, a stretch plus aging step has been inserted prior to warm rolling to facilitate nucleation of a refined intragranular precipitate prior to rolling. The intent of this is to produce a fine grain size and a large number of high angle grain boundaries capable of supporting a superplastic response, similar to that achieved previously [Ref. 5].

II. BACKGROUND

A. ALUMINUM ALLOY 2090

1. Development

Al alloys containing Li offer the promise of substantial weight savings in structural applications, particularly in the aerospace industry where weight reduction is an efficient means of improving aircraft performance. Each weight percent Li added to Al reduces the overall alloy density by 3% and increases the elastic modulus by 6%, allowing reduced cross-section of stiffness critical structural components in aircraft [Ref. 11,12].

Al-Li alloys have been in development since 1927 when the first United States patent was issued based on work in Germany with an alloy called Schleron [Ref. 13]. In 1941, Lebaron, working for Aluminum Company of America (Alcoa) applied for a patent on a proprietary Aluminum Lithium Copper alloy which was granted in 1950 [Ref. 14]. With the publishing of an Aluminum Lithium Phase Diagram in 1954 by Hardy and Silcock [Ref. 15], which is still widely accepted and used today, interest in the Al-Li-Cu system was revived at Alcoa. Eventually in 1958, trial production runs began at Alcoa of Al 2020 (Al-4.5Cu-1.1Li-0.5Mn). The Navy RA-5C Vigilante Fighter became the only production application for the alloy, where the material was utilized on some of the aerodynamic surfaces [Ref. 13]. However, concerns over the

fracture behavior of the alloy resulted in insufficient demand, and production ceased in 1969 with the replacement of the Vigilante aircraft.

In the early 70's the wave of the future appeared to be composites and it was projected that the use of Aluminum would diminish in years to come [Ref. 11]. However, the large capital investment in producing new facilities by aircraft manufacturers has sparked renewed interest in developing Al-Li alloys, with significant improvements in material properties evolving through intense research and development both by the aluminum industry, aircraft industry, and by academia [Ref. 16].

In 1981 Alcoa began the "Alithalite" project to develop low density replacements for several of their commercial alloys [Ref. 17]. In 1983 Alcoa began commercial product development of an Al-Cu-Li-Zr alloy, which was registered in 1984 with the Aluminum Association and assigned the designation 2090. This alloy was designed as the low-density replacement for 7075-T6X [Ref. 11]. Al-Li alloys in general are very prone to cracking, as are other high strength Al alloys such as 7050. In early 1986 Alcoa suspended production development work as acceptable quality for the Al-2090 products could not be attained routinely, and concentrated on research and development to improve ingot quality. As a result, production development was resumed,

with sheet, plate and extrusion products meeting design specifications [Ref. 16].

2. Precipitation Sequences

The exact precipitation sequences in Al 2090 are uncertain, particularly with respect to the various metastable phases which may precede the equilibrium phases in the system [Ref. 19]. Figure 1 summarizes the various morphologies of the possible metastable and equilibrium phases that have been reported [Ref. 9] for various microstructures. There is some controversy among authors as to the existence of the metastable phases T_1' and T_2', and since the temperatures used in this study (≥300°C) are well above the aging temperature used (163°C) to construct the schematic, it is anticipated that only the equilibrium phases will be present.

According to the Al-rich corner of the Al-Cu-Li phase diagram (Figure 2), first reported by Hardy and Silcock [Ref. 15], the composition of the alloy of interest here, namely 2.6 wt.pct.Cu and 2.0 wt.pct.Li, is such that the solvi for the equilibrium phases T_1 and T_2 are ≈ 520°C and ≈ 460°C, respectively. This is in agreement with Watson, who indicated that after isothermal precipitation at 500, 450, 400 and 350°C, the predominant phases would be T_1, T_1 plus some T_2, T_2 plus some T_1 and T_2, respectively [Ref. 18]. Thus, these phases would be expected to predominate in the microstructures at the temperatures used in this research. The T_1 (Al_2CuLi), which has a hexagonal structure, forms as coherent, hexagonal

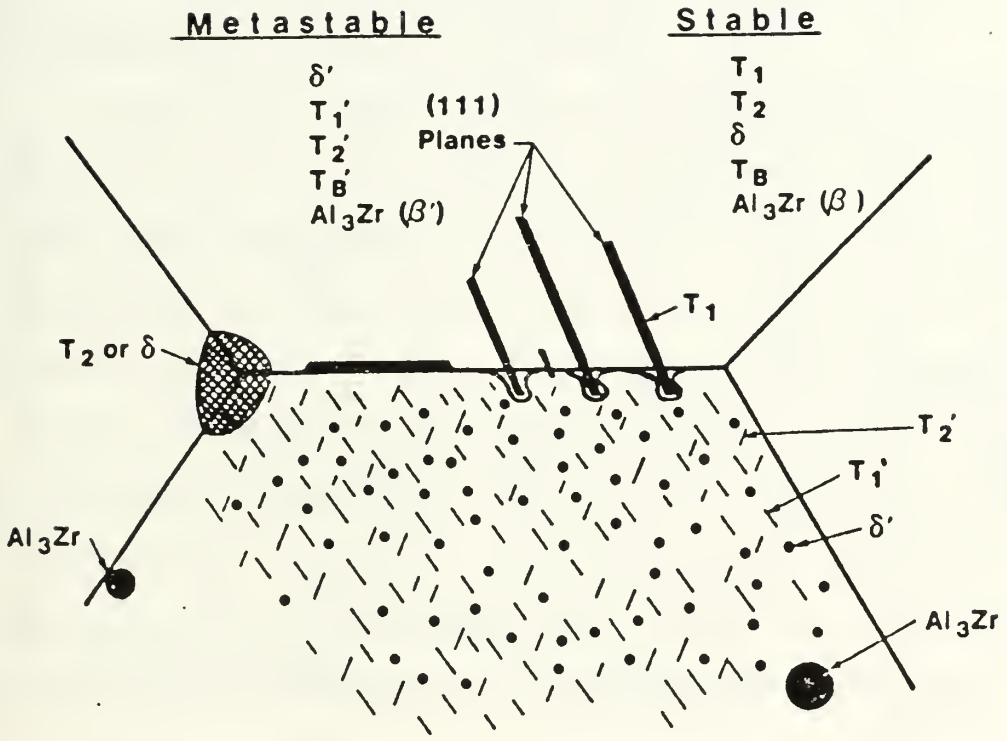

Figure 1. Schematic showing the typical morphology of precipitates in Al 2090 after a 6% stretch followed by aging at 163°C for 16 hours [ref. 9]. It is anticipated that the coherent, metastable phases (i.e., T_1', T_2', and δ') will not be present after aging at the temperature (350°C) used in this study.

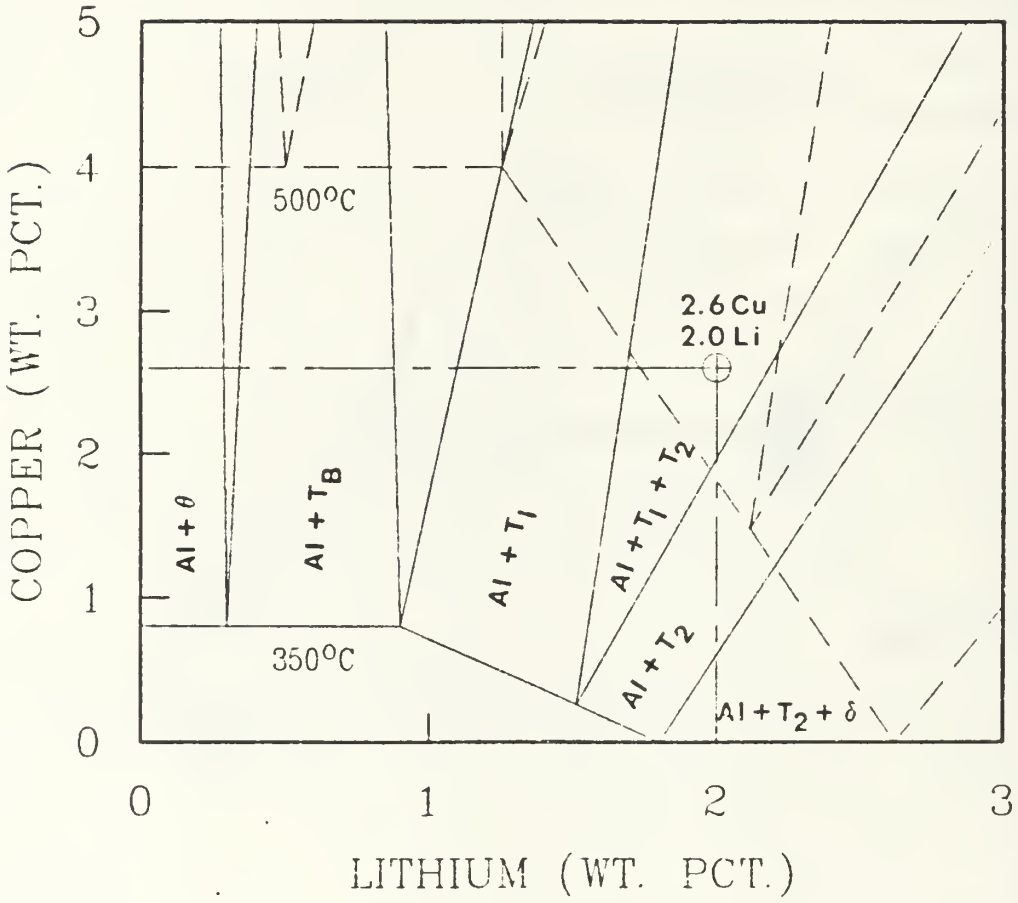

Figure 2. Phase boundaries of 350°C (——) and 500°C (---) isothermal sections of the ternary Al-Cu-Li phase diagram (Ref. 15).

platelets on (111) planes [Ref. 19]. The T_2 phase (Al_6CuLi_3), which has been reported to have an icosahedral structure, forms as non-coherent, blocky precipitates [Ref. 20]. Both phases tend to precipitate on grain boundaries and structural defects in grain interiors such as subgrain boundaries. Table 1 summarizes the composition and expected phases for the alloy and temperatures used in this research.

It is also important to mention that the alloy contains 0.12 wt.pct. Zr, which precipitates as $ZrAl_3$. Since this phase melts congruently at a temperature of 1577°C [Ref. 21], much greater than the melting point of the alloy, it is expected to be present during all stages of the processing in the metastable form as approximately spheroidal precipitates, vice the cuboidal equilibrium morphology [Ref. 21]. It has been recognized that the fine grain sizes necessary for superplasticity can be maintained by small ($\leq$ 0.5 wt.pct.) additions of Zr, which control recrystallization [Ref. 30].

B. SUPERPLASTICITY

Superplasticity is the ability of certain materials to exhibit large tensile elongations without localized necking. Materials which exhibit elongations of 200 percent or greater in tension are generally thought of as superplastic. The time devoted to the study of superplasticity and superplastic alloys has been relatively brief, with the first major review of unusual ductility effects appearing in 1962 by Underwood

TABLE I

PHYSICAL PROPERTIES OF ALLOY 2090

(a) Composition (Weight Percent):

	Cu	Li	Zr	Al
Specifications	2.4 -3.0	1.9 -2.6	0.08-0.15	Bal
This Alloy	2.56	2.03	0.12	Bal

(b) Predominant Intermetallic Phases:

Phase	T_1	T_2	β'
Compound	Al_2CuLi	Al_6CuLi_3	Al_3Zr
Structure	Hexagonal	Icosahedral	Cubic
Coherency	Coherent	Non-Coherent	Coherent
Habit Plane	(111)	-	(100)
Morphology	Platelike	Irregular	Spheroidal
Solvus	≈ 520°C	≈ 460°C	1577°C*

*Melting Temperature

[Ref. 22]. The reasons for these effects, the mechanisms, the corresponding microstructural evolution, and the potential applications were at that time unknown or not well understood [Ref. 23]. An explosion of research in the 60's and 70's has brought superplasticity to the forefront, and superplastic forming is now considered an economical means of manufacturing complex structures in one piece, thereby reducing weight, fasteners, and assembly costs [Ref. 12].

In order to facilitate superplastic forming, the following microstructural prerequisites [Ref. 24] must be developed through processing:

- A fine grain size, typically below 10um
- A uniformly distributed second phase precipitate, which is necessary to retard grain growth at the elevated temperatures
- Mobile high angle boundaries which may subsequently support grain boundary sliding (GBS), which most authors agree is essential to superplasticity [Ref. 25].

Grain boundary sliding (GBS) is a deformation mode consisting of the translation of grains relative to one another where the grains move in a direction parallel to the plane of the shared boundary. The sliding takes place in the absence of grain shape change [Ref. 26]. Thus the character of the boundaries, and especially their misorientation, is expected to control this phenomenon [Ref. 27].

Several methods are available to achieve the above required microstructure, two of which are commonly used in Al

alloys. The first of these is the so-called Rockwell method [Ref. 28], where the grain refinement is accomplished prior to deformation by discontinuous recrystallization. The basics of this process are solution treatment of the material, to dissolve precipitates, followed by quenching. The material is then overaged to create precipitate particles which act as nucleation sites for recrystallizing grains. Next the material is warm rolled to introduce defects into the alloy to promote recrystallization. The rolled material is then heated to the recrystallization temperature, whereby complete recrystallization takes place by conventional nucleation and growth processes. [Ref. 29]

The second method, developed by Alcan for Supral (Al-Cu-Zr) alloys, does not incorporate a separate recrystallization heat treatment [Ref. 30]. This method utilizes dynamic continuous recrystallization, which occurs prior to and during the initial stages of hot deformation, to produce a fine-grained, superplastic microstructure. The mechanism of continuous recrystallization is proposed to consist of the development of a subgrain structure and subsequent coalescence of these subgrains to form grains [Ref.31]. This latter method is similar to the thermomechanical processing developed at the Naval Postgraduate School, and utilized for this current research, the major difference being the lower temperatures used for processing and deformation [Ref. 5].

C. OBJECTIVE OF THIS RESEARCH

With the introduction of "Alithalite" Aluminum Alloy 2090 by Alcoa in 1984 as a commercial low density replacement for the successful 7075 series aluminum alloys, considerable effort has centered on determining the superplastic properties of this alloy. The current level of understanding of second phase precipitation in Al 2090 indicates that to obtain a refined microstructure by the method used for the Al-Mg alloy, it is necessary to promote intragranular precipitation. Thus, a stretch plus age treatment prior to thermomechanical processing may provide the uniform distribution of particles desired for producing a refined microstructure.

Consideration of the phase diagram [Ref. 14] indicates that aging at 350°C will produce a mixture of T_1 and T_2 precipitates. It was anticipated that the non-coherent T_2 phase would perform a similar role to the β phase in the Al-Mg alloys. In the Al-Mg alloy, precipitation is sufficiently rapid that the initial subgrain size produced during the early rolling passes is determined by the spacing of the β phase precipitates [Ref. 5]. A large volume fraction of uniformly distributed non-coherent particles which precipitate simultaneously with the formation of a substructure controls the final continuously recrystallized grain size [Ref. 6]. The combination of the temperature employed (300°C) and the highly refined grain structure also dictates that cavitation is suppressed in the material [Ref. 4].

Previous investigations at NPS on Al 2090 have concentrated on varying the basic thermomechanical processing schedule developed for the Al-Mg-X alloys. Spiropoulos [Ref. 32] centered his research on a TMP schedule involving homogenization, upset forging, 10% cold work, low temperature aging, and subsequent rolling and tensile testing, utilizing various rolling temperatures, reheating intervals and tensile testing temperatures. Regis [Ref. 33] continued the investigation, using a similar TMP schedule without the aging prior to rolling. Neither effort resulted in superplastic elongations approaching those which had been attained in the Al-Mg-X alloys. Limited microstructural analysis failed to reveal the reasons for the poor superplastic response.

Recently, Watson and Bennetch, of Reynolds Aluminum Co, reported achieving elongations in excess of 1000% utilizing a TMP schedule whose primary feature was an aging treatment of 350°C for four hours. Thus, this work is centered on a TMP utilizing a higher temperature aging process than that employed by Spiropoulos. The process was also, however, designed to promote T_1 and T_2 formation prior to rolling.

III. EXPERIMENTAL PROCEDURE

A. MATERIAL

The composition of the Al 2090 alloy studied in this investigation is Al-2.56Cu-2.03Li-0.12Zr (wt.pct.). The material was provided in the form of rolled plate approximately 51 cm long, 31 cm wide and 4 cm thick in a T8A41 tempered condition. (i.e. The material had been solution treated, cold-worked, artificially aged, and anodically coated [Ref. 34]).

B. PROCESSING

The overall thermomechanical processing (TMP) scheme is summarized in Figure 3 and the details are as follows:

1. Solution Treatment and Forging

This step is designed to produce a uniform starting condition by dissolving the soluble precipitates in the alloy. Blocks 41mm x 43mm x 51 mm previously sectioned from the material were held at 540°C for 2 hours, well above the solvi for the T_1 and T_2 phases. This temperature is insufficient to re-dissolve the Al_3Zr dispersoid formed during casting. The blocks were then upset forged in the longitudinal direction, or in the short transverse direction, as shown in Figure 4, in a Baldwin-Tate-Emery universal testing machine between two platens heated to 480°C (maximum allowable temperature of the

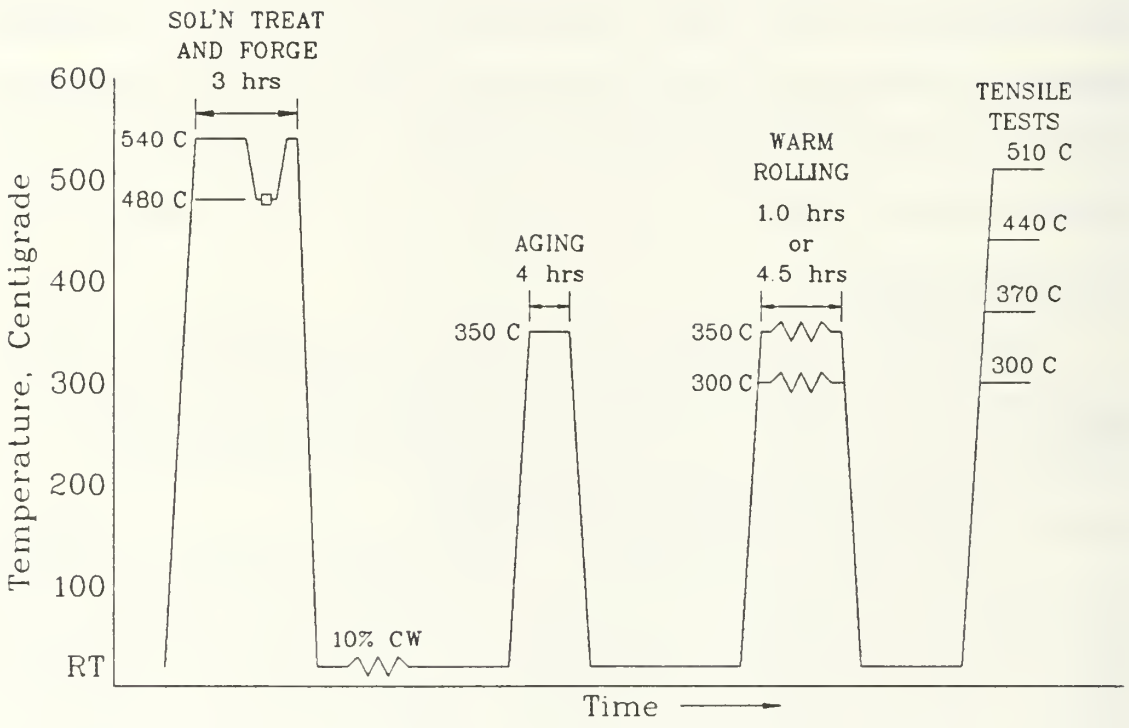

Figure 3. Schematic representation of the thermomechanical processing schedule utilized on Alloy 2090.

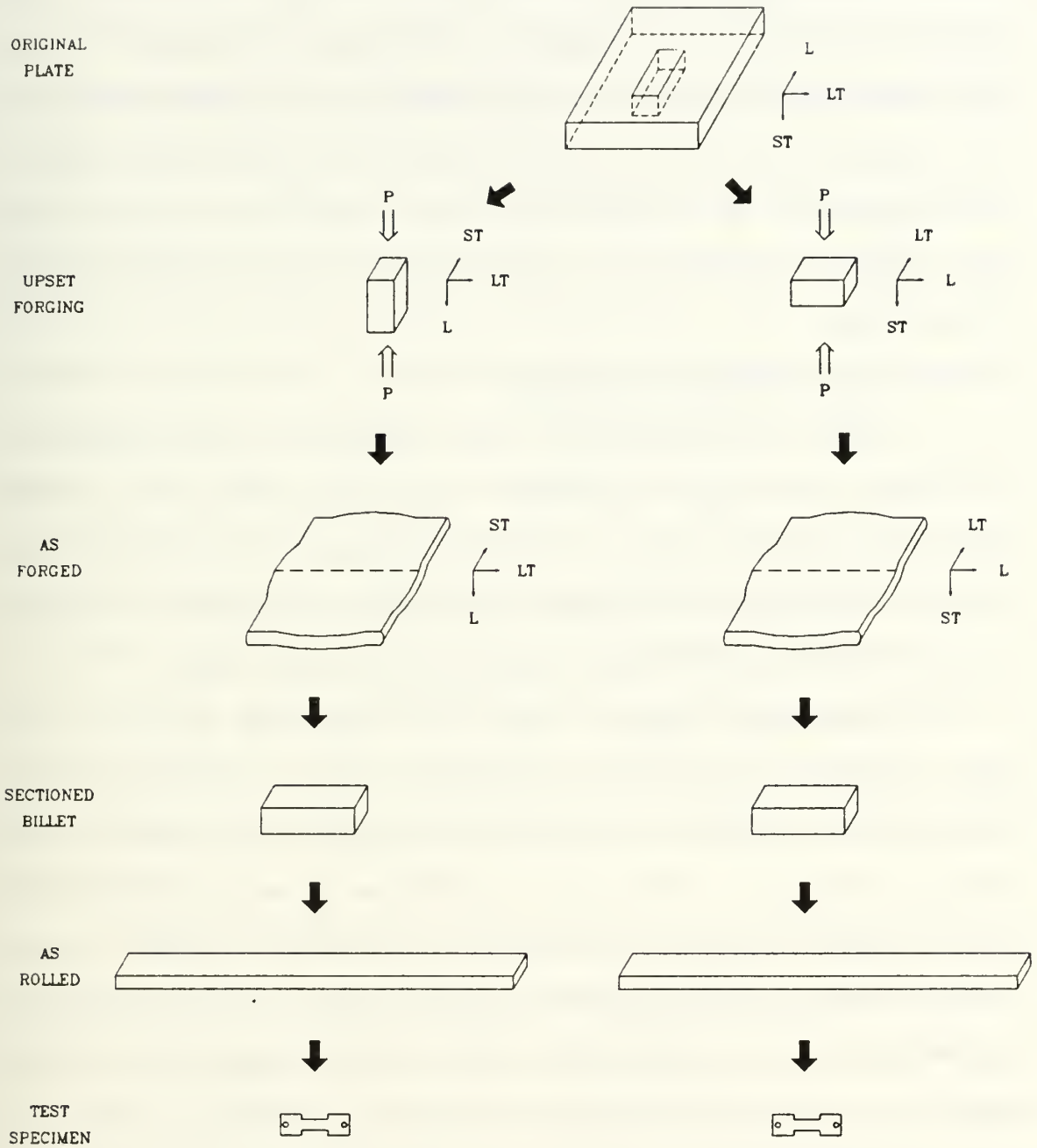

Figure 4. Plate to test specimen geometry. Rolling parallel to the original plate short-transverse direction is not represented due to cracking during attempts to roll.

platen material), to a thickness of about 25.4 mm. The resultant billet was reheated and solution treated for an additional hour at 540°C and subsequently cold water quenched. The forged billets were then sectioned to provide two pieces. The subsequent TMP process could be conducted to investigate the effects of rolling parallel to each of the original plate directions.

2. Cold Working and Aging

Each sectioned billet was rolled to a 10% reduction, achieving a nominal thickness of about 24mm, on a FENN laboratory scale rolling mill. The purpose of this cold work was to introduce sufficient dislocations for the T_1 and T_2 phases to precipitate upon during subsequent aging.

Artificial aging, which was conducted at 350°C for four hours, was chosen to coincide with the aging used by Watson and Bennetch in achieving elongations in excess of 1000 percent [Ref 17]. The T_2 was desired as it was believed that the T_2 could perform the role of the β phase in the Al-Mg-X series, namely limiting substructure growth by stabilizing the existing low angle boundaries such that subsequent deformation would promote the development of high angle boundaries.

3. Warm Rolling

Warm rolling is the critical step in the TMP, performed under a combination of parameters intended to convert the microstructure into one capable of supporting superplasticity. It is accomplished by a series of rolling

and annealing treatments designed to promote continuous recrystallization, which is a process involving the recovery of dislocations introduced during the rolling such that high angle grain boundaries are formed.

Warm rolling was conducted at two different temperatures of 300°C and 350°C. All billet sections were preheated to the rolling temperature for 30 minutes. Reheating intervals of either four or 30 minutes duration were subsequently used between each rolling pass. A 0.5 inch thick steel plate was used as a heat sink in the furnace to facilitate heating the material to the desired isothermal rolling temperature. Each rolling pass took approximately 20 seconds, with the roll surfaces at ambient temperature. A total strain of 2.5 was achieved in eight rolling passes of approximately 2.5mm reduction (10% of original billet thickness) per pass, resulting in a final rolled sample thickness of 1.8 to 2.0 mm.

Warm rolling was attempted on each of the sectioned billets such that TMP rolling direction would be parallel to each of the as-received plate directions, as illustrated in Figure 4. However, attempts to roll the billet sectioned parallel to the original plate short transverse direction resulted in cracking running in the long transverse direction.

C. TENSILE TESTING

Mechanical properties of the thermomechanically processed material were obtained using samples with the following gage dimensions: 12.7mm length, 5.1mm width, 1.8-2.0mm thickness, and a 1.6mm shoulder radius [Ref. 33]. These were machined from the as-rolled material such that the tensile test axis was parallel to the prior TMP rolling direction. Tension testing on material from each of the TMP process variants was conducted at 300°C, 370°C, 440°C and 510°C at a constant crosshead speed corresponding to an engineering strain rate of 6.67×10^{-3} sec^{-1} on an Instron model TTD universal testing machine utilizing a Marshall model 2232 three zone clamshell furnace to heat the specimens to test temperature. Tension testing data was corrected to compensate for the decrease in true strain rate with increasing strain. Details of this compensation method have been outlined previously [Ref. 35].

D. METALLOGRAPHY

In support of this research optical microscopy was conducted on the material both before and after warm rolling. Specimens were cold mounted, mechanically polished, and etched for 20 sec in Kellers etchant [Ref. 36] Metallography was conducted utilizing a Zeiss ICM 405 optical microscope with a 35mm camera.

Transmission electron microscopy studies were performed on the material in the same conditions as above and also at

the onset of tensile testing for the material rolled at 300°C with 30 minute reheating intervals. For this latter condition, material was obtained from grip sections of tensile samples. Specimens were removed from bulk material such that the foil normals were parallel to the rolled sheet normal. Electrothinning was accomplished in a solution of 20% nitric acid in methanol cooled to -15°C at an applied DC voltage of 17 V, resulting in currents of approximately 0.3 amps and a perforation time of ≈ 100 seconds. The thin foil specimens were examined using a JEOL 100 CX-II transmission electron microscope operating at an accelerating voltage of 120 kV.

IV. RESULTS AND DISCUSSION

A. MECHANICAL PROPERTIES

Three variables in the thermomechanical processing schedule were investigated in this research, namely processing (rolling) direction with respect to the rolling direction of the as received plate, the reheating interval between rolling passes, and the tensile testing temperature. Results are summarized in tabular form in Table II, and graphically in Figures 5 and 6. Peak ductilities were obtained at a tensile testing temperature of 370°C for all conditions. Lower ductility was attained at lower and higher temperatures with the exception of material processed with four minute reheating intervals and with the final rolling direction parallel to the original plate rolling direction (sequence B on Figure 4). For this case a slight increase in ductility was noted when the tensile test temperature was increased from 440°C to 510°C (Figure 6). This increase in ductility at higher temperatures may be due in part to data uncertainty arising from the difficulty associated with testing alloy 2090 at elevated temperatures, since the stress required for deformation is extremely low at temperatures over 400°C. Hence specimen failure occurs at extremely low stresses (a few PSI), where other factors such as specimen alignment or minor imperfections in the test specimen may cause premature

TABLE II

SUMMARY OF DUCTILITY DATA

PROCESSING CONDITION			ELONGATION (PCT.)			
Rolling Temperature (°C)	Reheating Time (min)	Rolling Direction *	Test Temperature (°C)			
			300	370	440	510
300	4	L.T.	84	154	123	117
300	30	L.T.	103	215	133	132
350	4	L.T.	71	144	132	98
350	30	L.T.	64	165	152	105
300	4	R.D.	84	121	108	129
300	30	R.D.	102	245	142	124
350	4	R.D.	87	142	91	112
350	30	R.D.	87	192	148	104

Strain rate for tensile testing = 6.67×10^{-3} S^{-1}

* - Warm rolled parallel to the long-transverse direction (L.T.) and to the rolling direction (R.D.) of the original as-received plate.

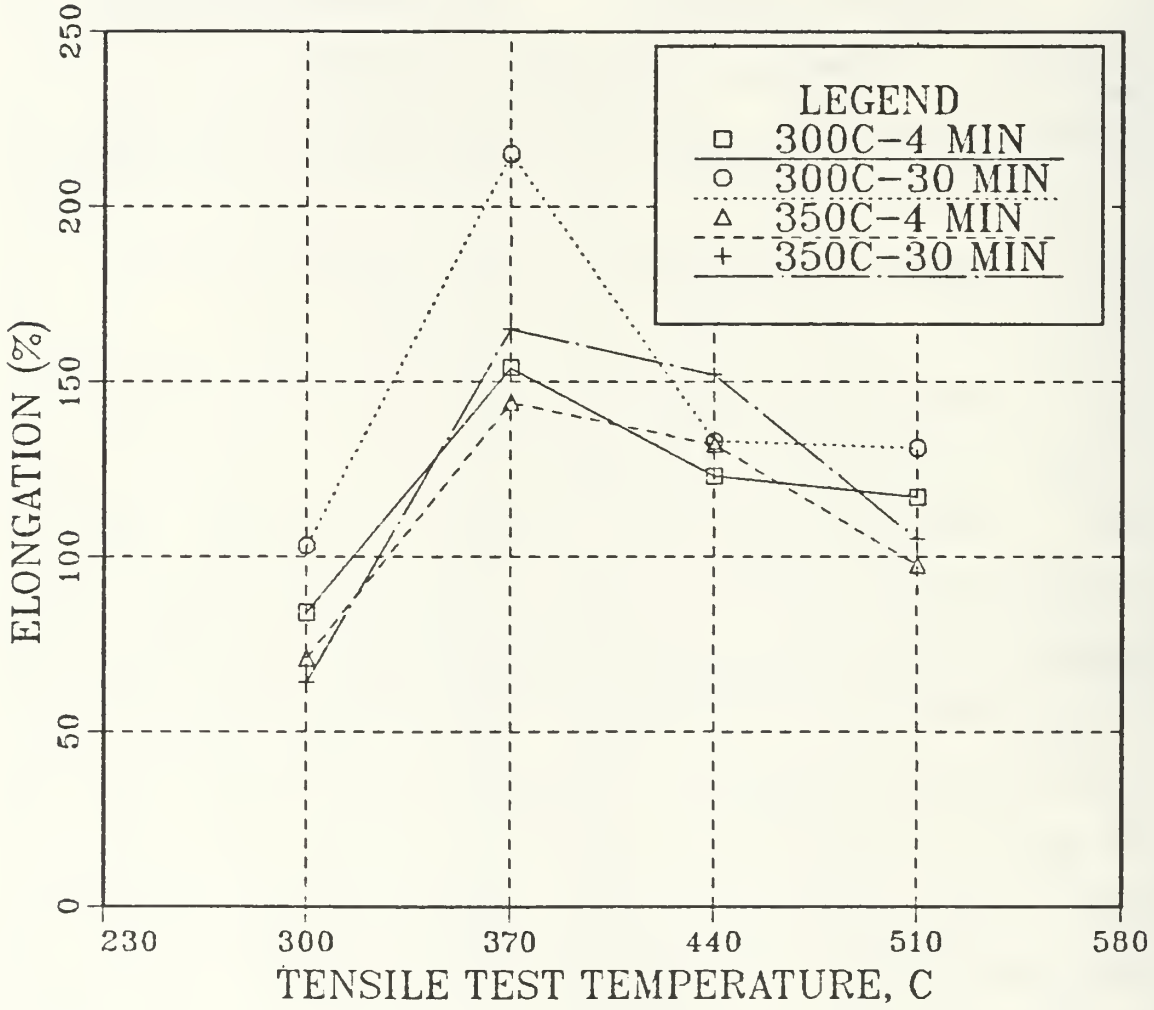

Figure 5. Ductility vs. Tensile Test Temperature for various TMP schedules shown in the legend. Rolling direction was parallel to the original plate long-transverse (LT) direction.

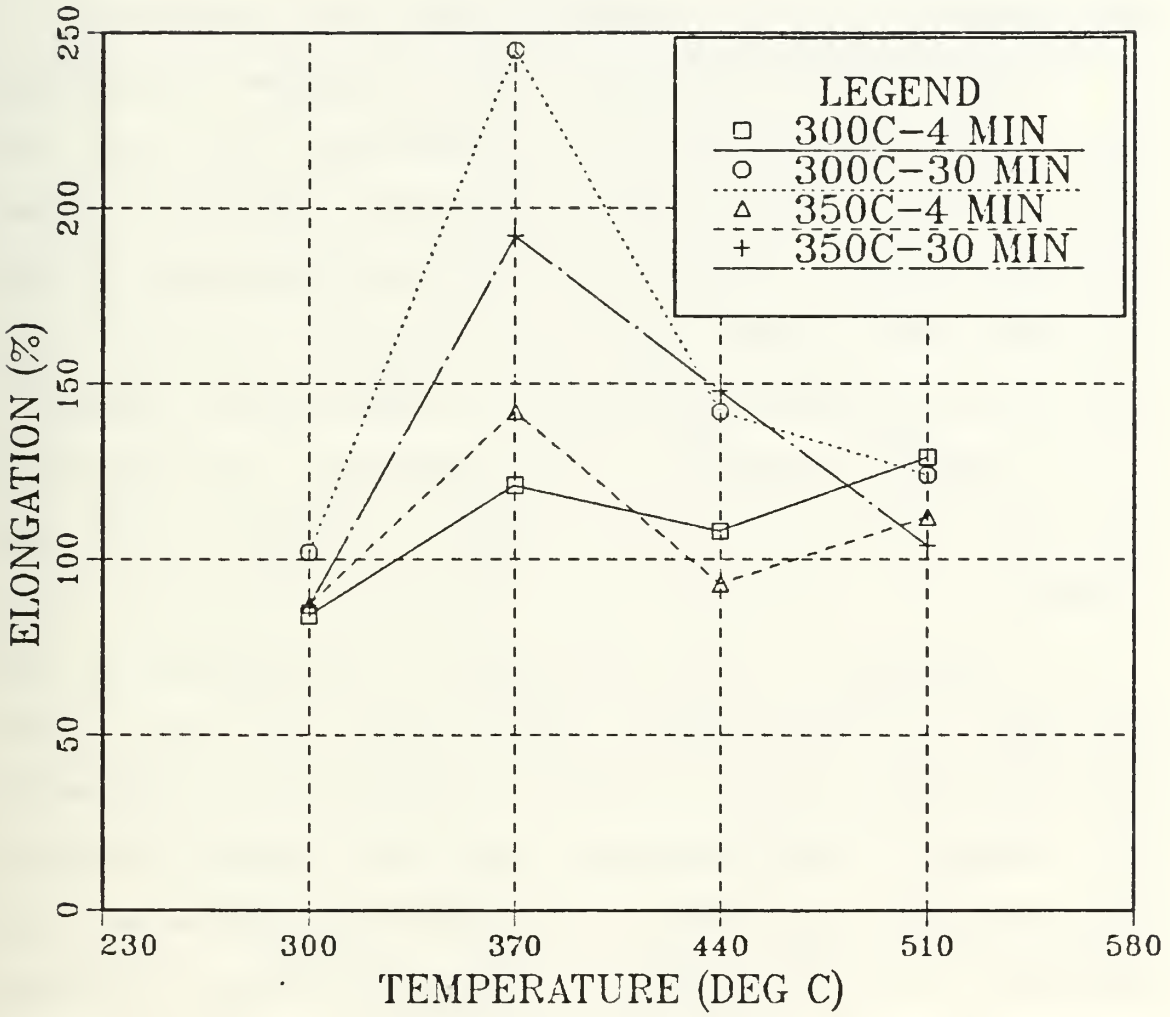

Figure 6. Ductility vs. Tensile Test Temperature for various TMP schedules shown in the legend. Rolling direction was parallel to the original plate longitudinal direction (L).

failure. In previous work [32, 33], it was concluded that this decrease in ductility with an increase in test temperature was a result of microstructural coarsening. The data presented here are consistent with that conclusion.

Figures 5 and 6 also reveal that the highest ductilities achieved at the optimum test temperature of 370°C are substantially less for shorter reheating intervals between reduction passes. In the previous investigations, it was concluded that short reheating intervals do not allow sufficient time for the recovery of dislocations, generated by the rolling, to recover to the boundaries. Data obtained from this present research is again consistent with this finding.

A comparison of the affects of orientation of the processed rolling direction with respect to that of the original plate is shown in Figure 7 for material processed at 300°C with 30 minute reheating intervals. Slight increases in ductilities were noted at all test temperatures with the exception of testing at 510°C. This insignificant increase suggests that, at least macroscopically, that the solution treatment and upset forging has succeeded in removing most anisotropy from the original plate.

Although moderate superplasticity was achieved (215-245 percent maximum elongations) these were still far below those reported by Watson [Ref. 18] and others for material processed and tested at elevated temperatures, and were also well below

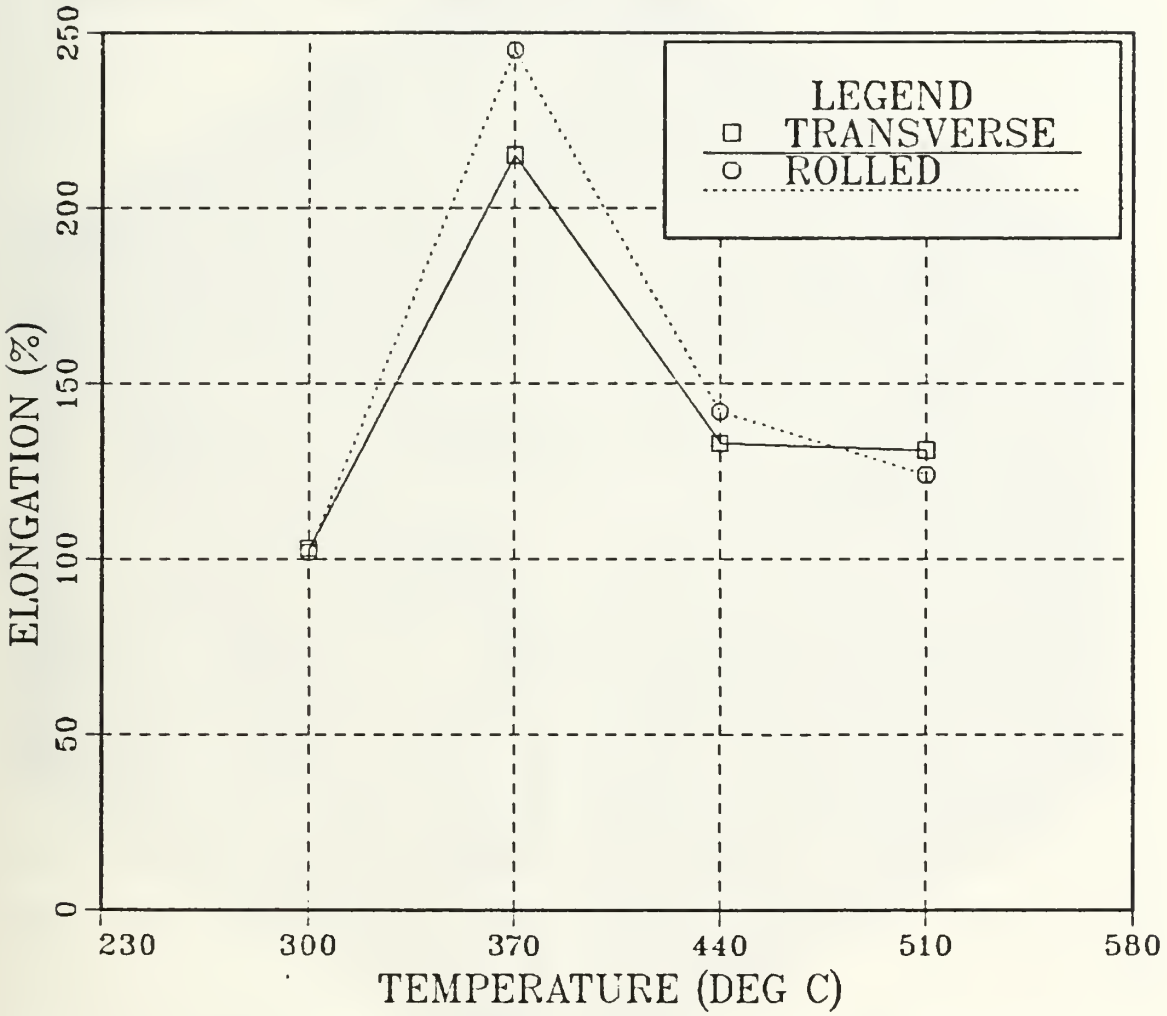

Figure 7. Comparison of Ductility vs. Tensile Test Temperature for material rolled at 300°C with 30 minute reheat intervals between passes. Data is presented for each of the two warm rolling directions with respect to the rolled direction of the original plate.

those achieved in the Al-Mg-X systems utilizing similar TMP schedules here at NPS. This prompted a microstructural study utilizing both optical and transmission electron microscopy to determine the evolution of the microstructure processed by this TMP.

B. MICROSTRUCTURAL CONDITION PRIOR TO ROLLING

Solution treatment, upset forging, cold work and subsequent aging in accordance with the TMP has created an inhomogeneous, large-grained microstructure with both inter-granular and intra-granular precipitates as shown in the optical micrographs in Figure 8. There appear to be remnants of the microstructure of the as-received plate here, as the grains tend to be aligned perpendicular to the short transverse direction of the original plate (Figure 9a). This could reflect mechanical fibering or long range segregation in the original plate. Figures 9a and 9b also reveal that the discrete precipitates on the grain boundaries have associated precipitate free zones (PFZ) which are wider in the plane section.

A more detailed investigation using TEM correlates the observations in the optical microscopy. Figure 10 shows the grain boundary is decorated with a precipitate, identified as T_2 based on its morphology [Ref. 20] and on the phase diagram as proposed by Hardy and Silcox [Ref. 15]. The principal precipitate within the grain interiors is identified as T_1

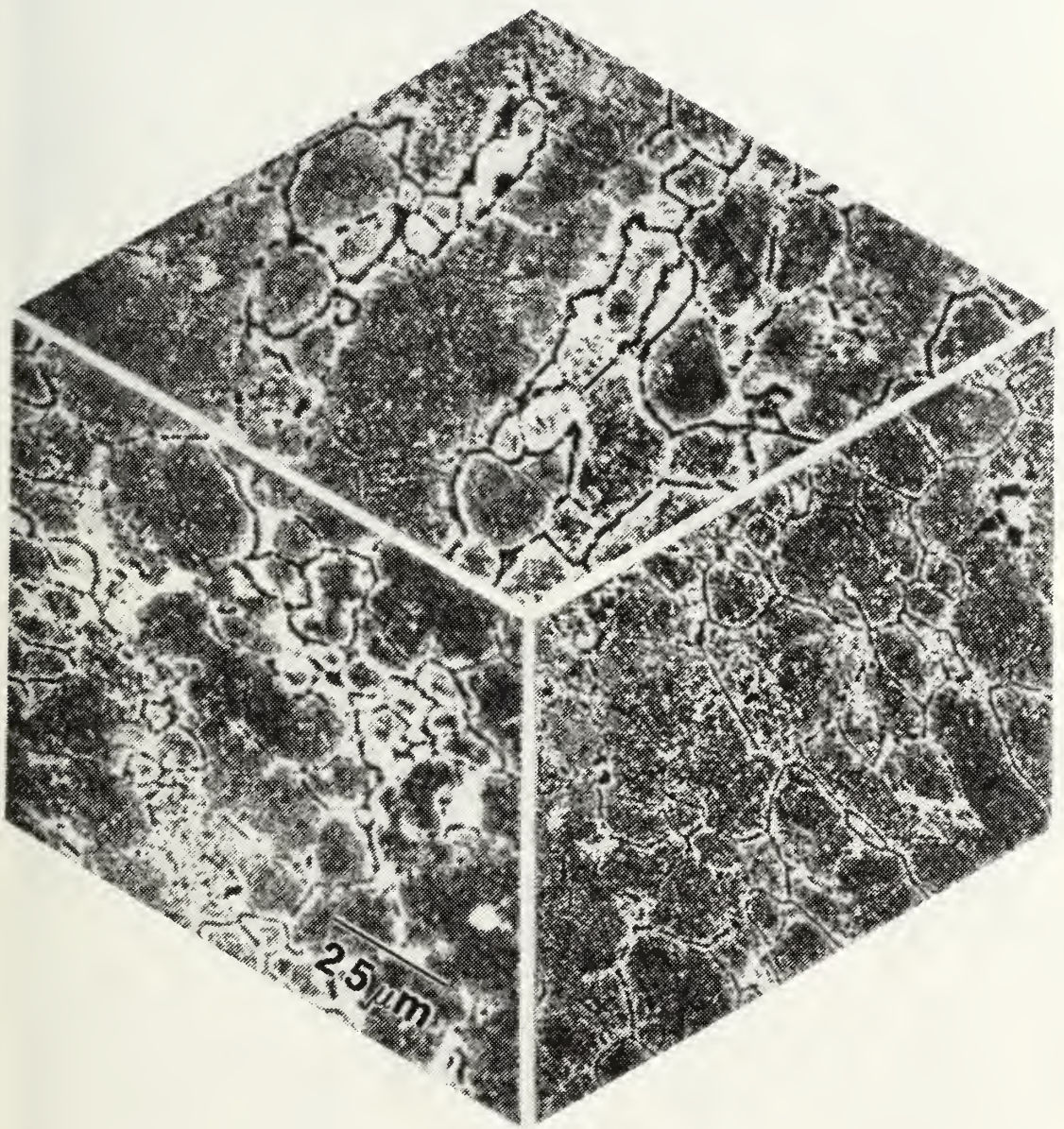

Figure 8. Tri-planar optical micrograph of Alloy 2090 in the as-forged plus aged (4 hr at 350°C) condition. An even distribution of intragranular precipitates and decoration of grain boundaries with intergranular precipitates is apparent.

(a)

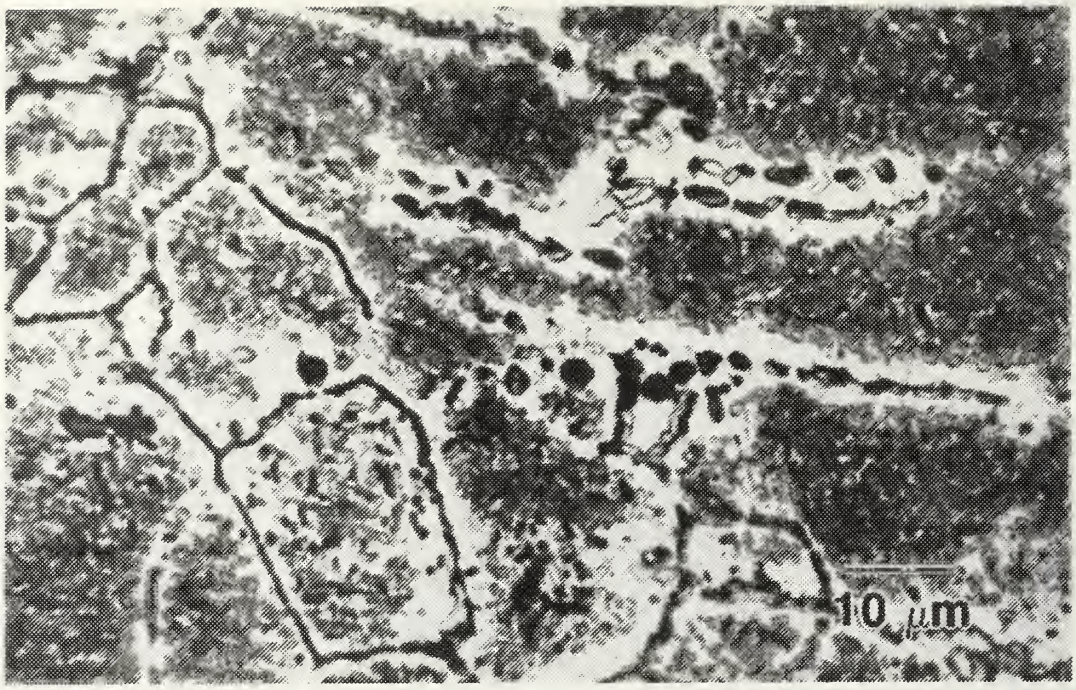

(b)

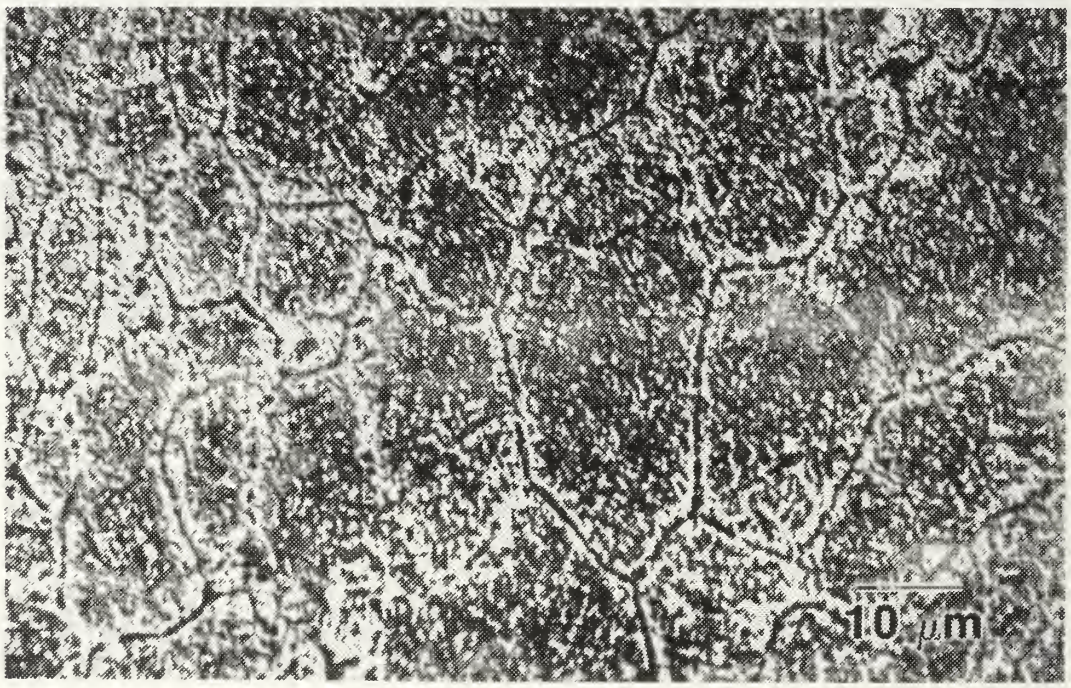

Figure 9. Plane section (a) and long-transverse section (b) optical micrographs of Alloy 2090 in the as-forged and aged condition. Note the PFZ's near the grain boundaries.

(a)

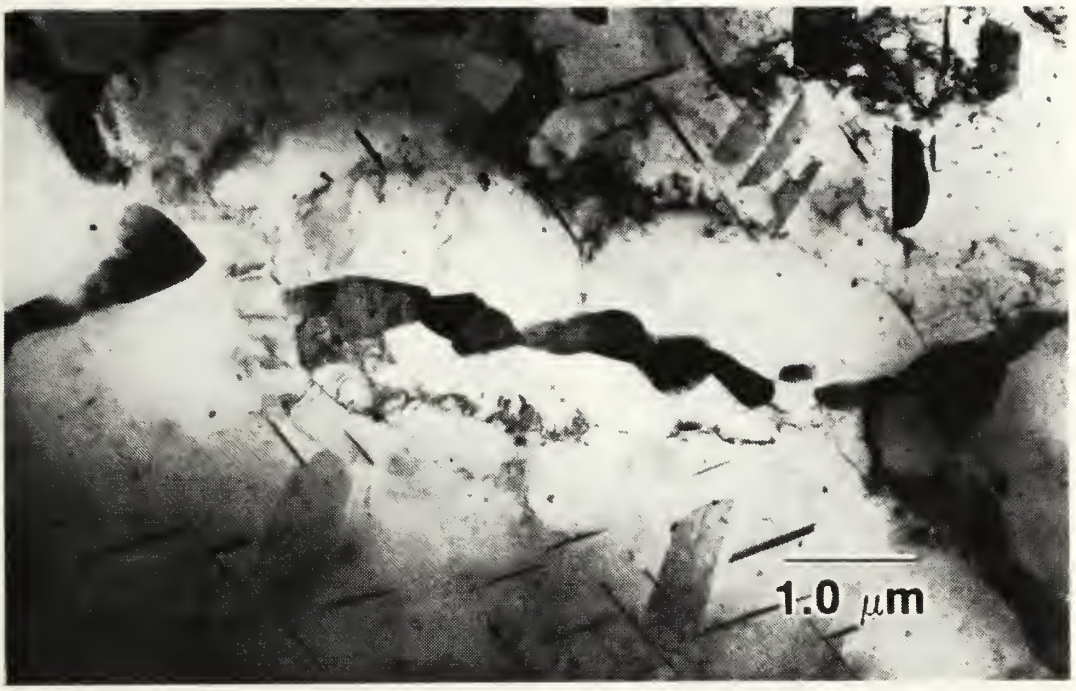

(b)

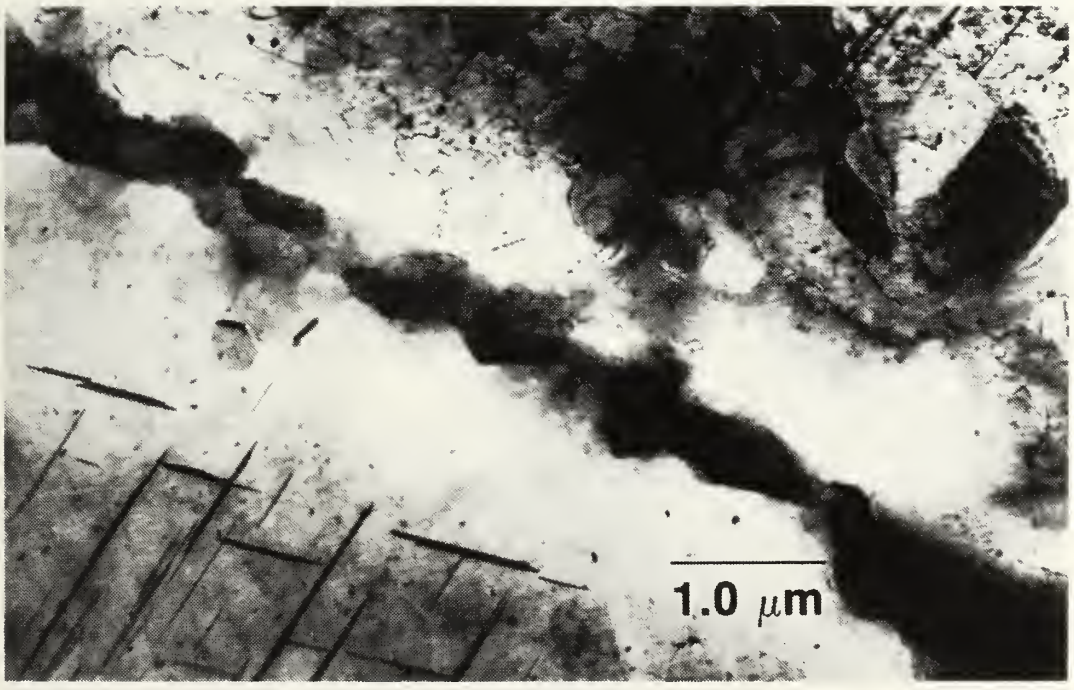

Figure 10. Bright field TEM micrographs from plane section of alloy 2090 in the as-forged plus aged condition: (a) T_2 decorates the grain boundary, while T_1 has precipitated intragranularly. In (b) a T_1 PFZ is clearly visible.

(Al_2CuLi) based on its plate like morphology and the (111) habit plane with respect to the matrix [Refs. 9,19]. The grain boundary precipitate has denuded the adjacent matrix of lithium, or copper, or both, resulting in a (PFZ) in which T_1 is absent adjacent to the grain boundary, as seen in Figure 10. The T_1 has also precipitated upon the subgrain boundary, also on the (111) plane as shown in Figure 11a. Figure 11b shows the morphology of the intragranular T_1 phase, as well as small spheroidal, uniformly distributed Al_3Zr precipitates.

C. MICROSTRUCTURAL CONDITION AFTER ROLLING

Optical triplanar micrographs of Al 2090 following forging, aging, and warm rolling to a true strain of 2.5 at 300°C, with a reheating interval of 30 minutes between rolling passes, show that a uniform, fine second phase precipitate distribution has been achieved, with the exception of isolated examples of very coarse precipitate stringers aligned in the rolling direction (Figure 12). The grain structure is now indiscernible, and there is no evidence of the previously noted PFZ's. These precipitates tend to run perpendicular to the original plate short transverse direction (Figure 13) and therefore suggest that these are remnants of the precipitates formed on the prior grain boundaries. The existence of such heterogeneities gives insight as to why cracking was observed during attempts to roll the forged billet in a direction parallel to the original short transverse direction. Such

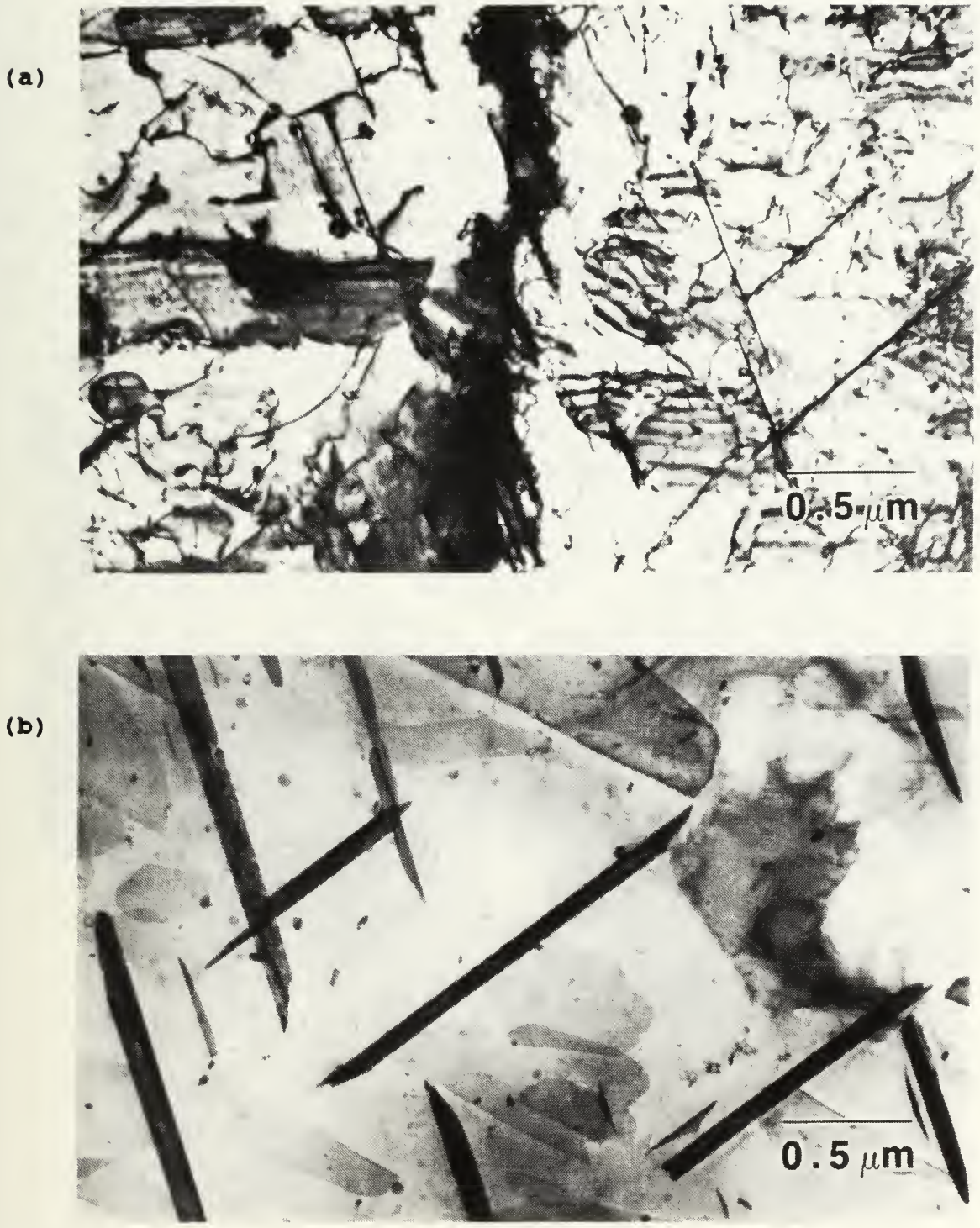

Figure 11. Bright field TEM micrographs from plane section following aging at 350°C showing, (a), T_1 precipitation at a grain boundary along (111) planes, and (b), the plate-like morphology of the intragranular T_1. Note the uniform distribution of small, spheroidal Al_3Zr precipitates.

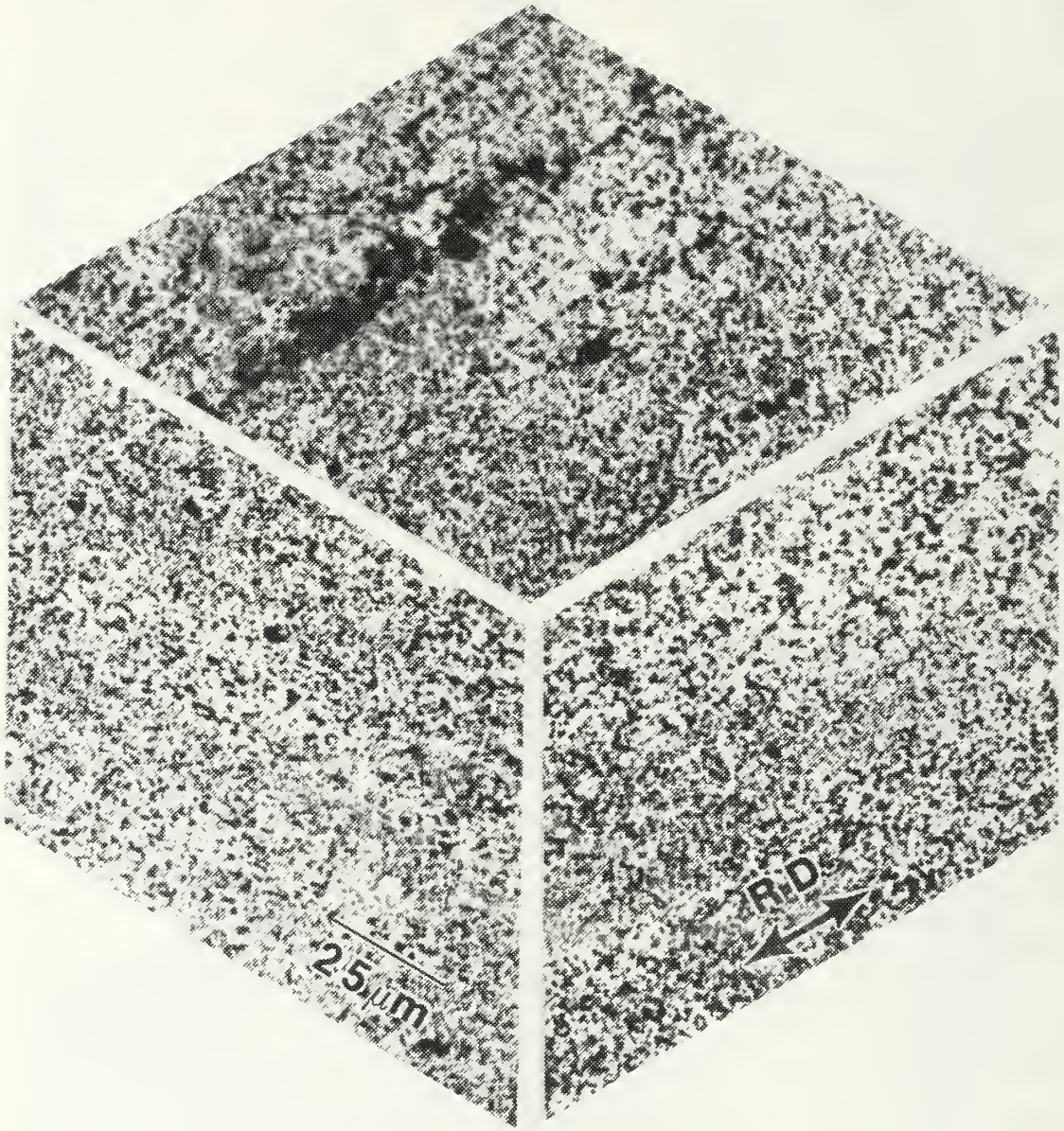

Figure 12. Optical tri-planar micrograph of alloy 2090 forged and aged, and then rolled to a true strain of 2.5 at 300°C with 30 minute reheating intervals between rolling passes.

(a)

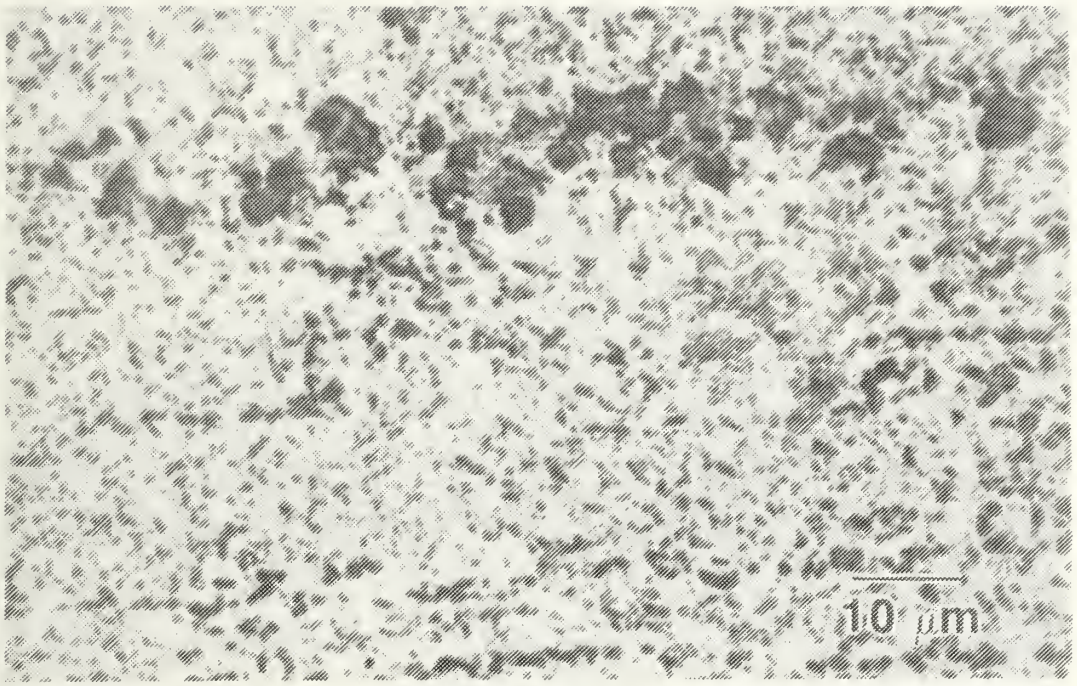

(b)

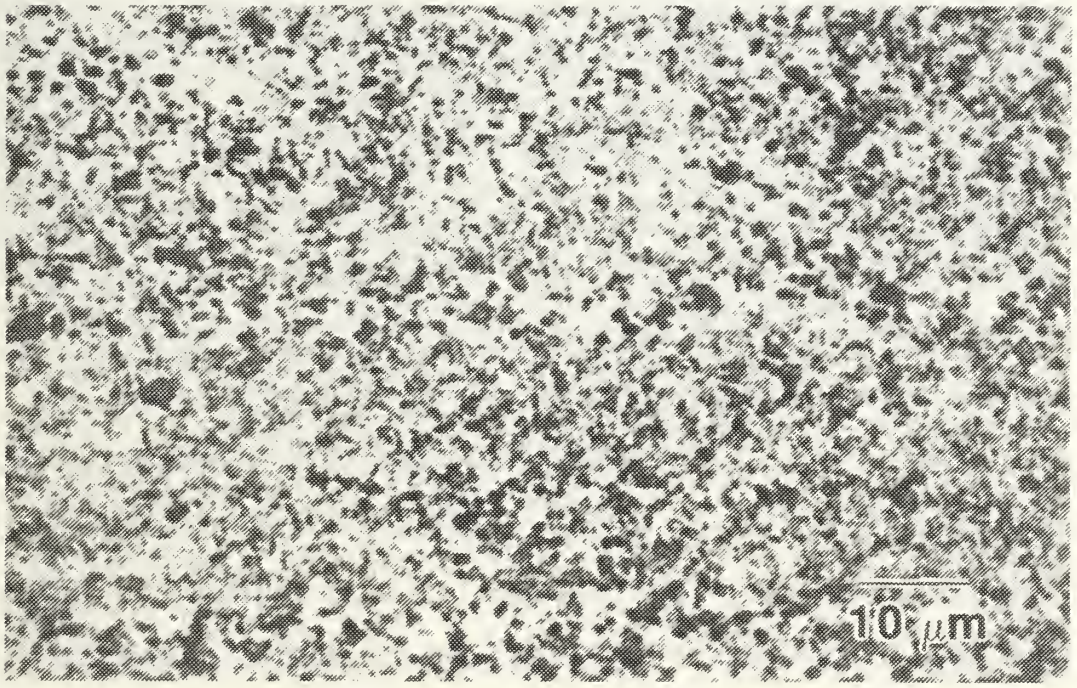

Figure 13. Plane section (a) and long-transverse direction (b) optical micrographs of alloy 2090 rolled to 2.5 true strain at 300°C with 30 min reheat intervals. Precipitates appear to be "strung out" along the rolling direction in (a).

large heterogeneities may also develop large deformation zones around them, and may therefore tend to promote subsequent nucleation of recrystallized grains and subsequent grain growth, affecting the resultant mechanical properties.
res 14 and 15 show the affects of increased rolling temperature on the microstructure of the 2090 alloy for material rolled at 350°C with 30 minute reheating intervals. Precipitate size has increased over that rolled at 300°C, but overall volume fraction seems to have remained the same. This again is consistent with the results reported previously [Refs. 32, 33].

In order to fully characterize the microstructure at the conclusion of thermomechanical processing, TEM studies were conducted on the material rolled at 300°C with 30 minute reheating intervals between passes. The material warm rolled in a direction parallel to the transverse direction of the original plate and tested at a temperature of 370°C was chosen so a direct comparison with previous work on the Al-Mg-X series could be made.

The microstructure of the as-rolled material varies somewhat, with three distinct morphologies being intermixed with the same foil. The first, illustrated in Figure 16a reveals a heavy dislocation substructure around a large, blocky precipitate. Looking at the matrix in more detail in Figure 16b, reveals a network of substructure boundaries believed to be predominately low angle in nature based on

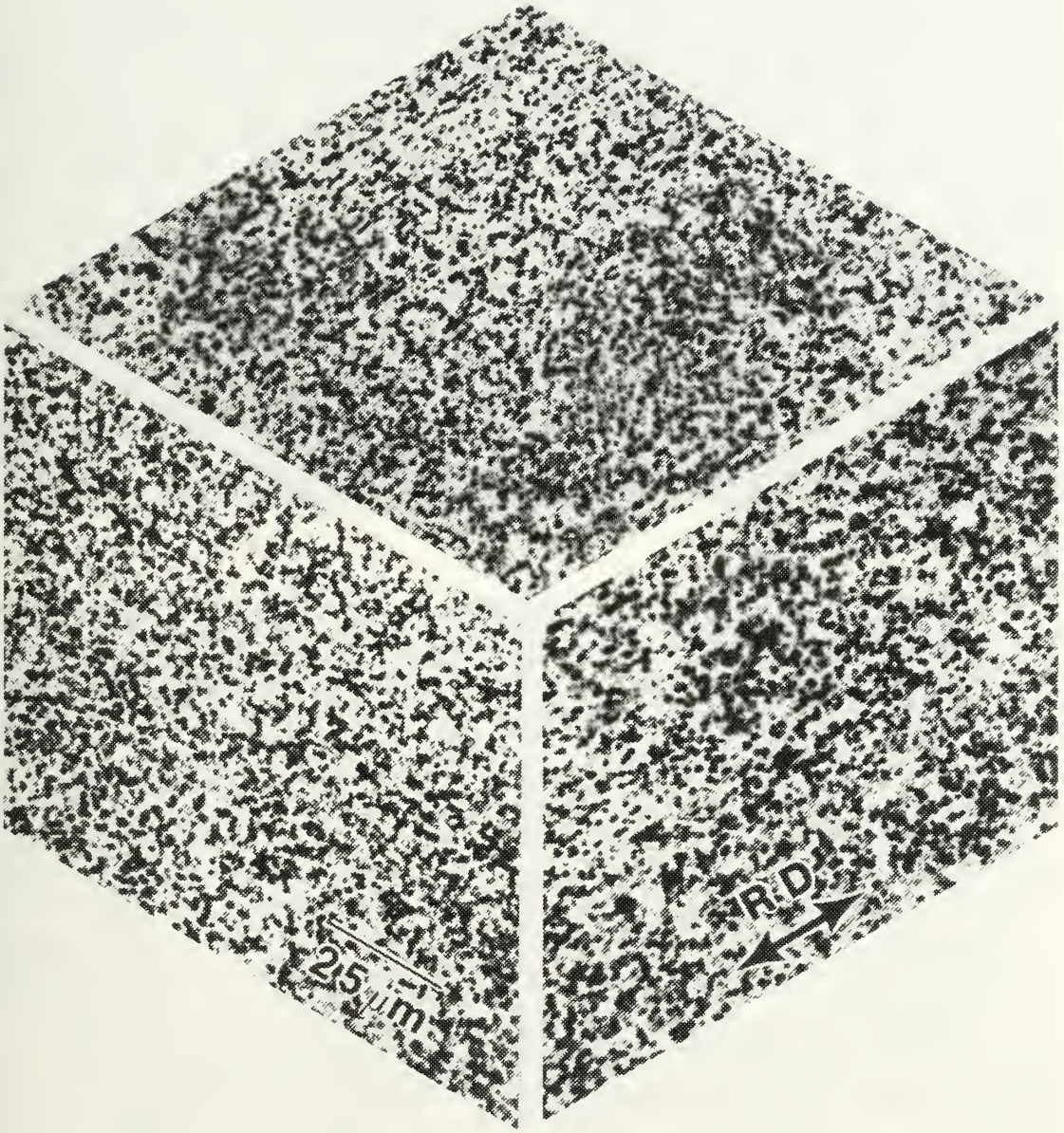

Figure 14. Optical tri-planar micrograph of alloy 2090, forged and aged and then rolled to a true strain of 2.5 at 350°C with 30 min reheating intervals between rolling passes. The evenly distributed precipitates are coarser than those in the material rolled at 300°C (Figure 10).

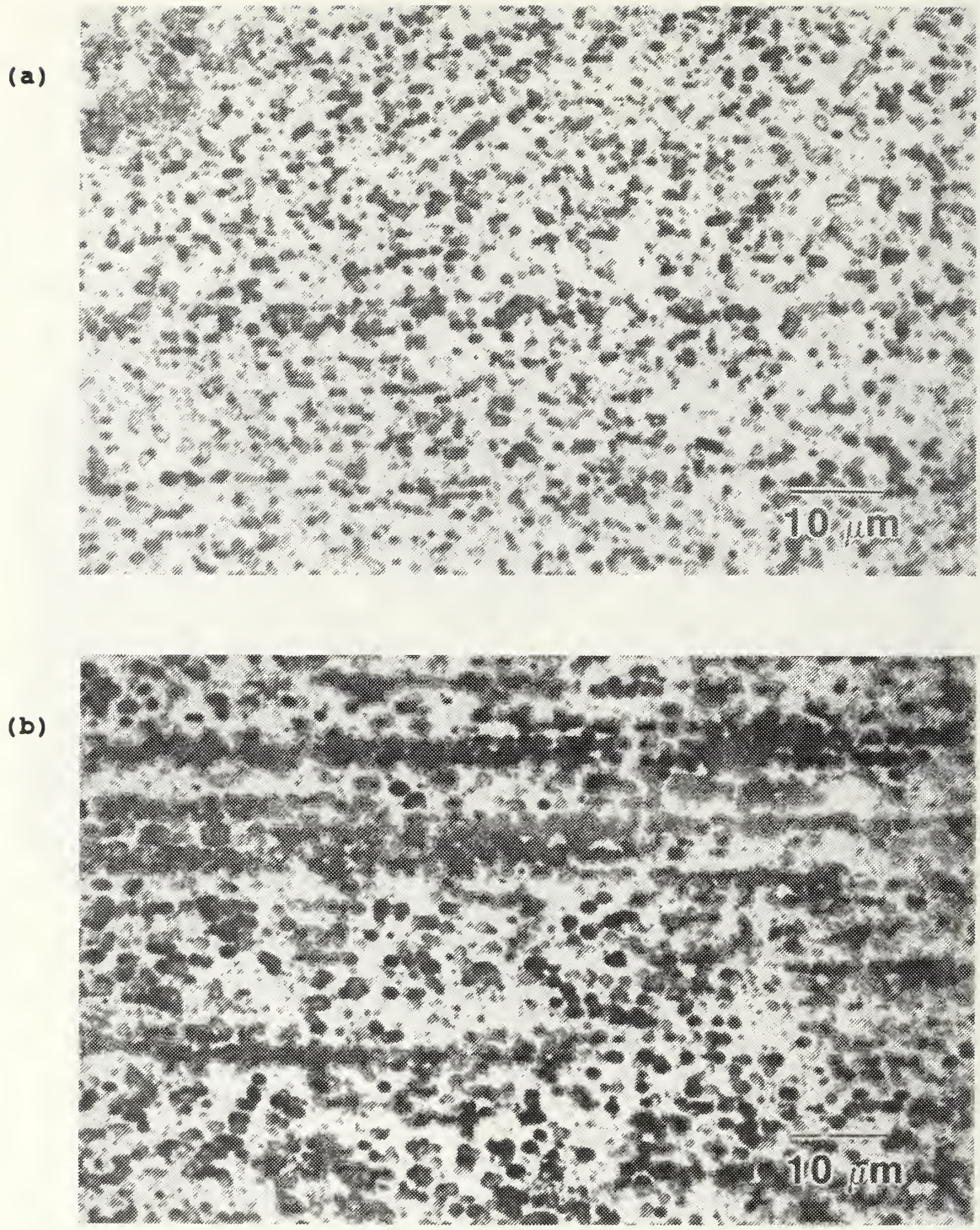

Figure 15. Plane section (a) and long-transverse section (b) optical micrographs of alloy 2090 following rolling at 350°C to a true strain of 2.5 with 30 min reheating intervals between passes. The microstructure is coarser than that noted in material rolled at 300°C (Figure 13).

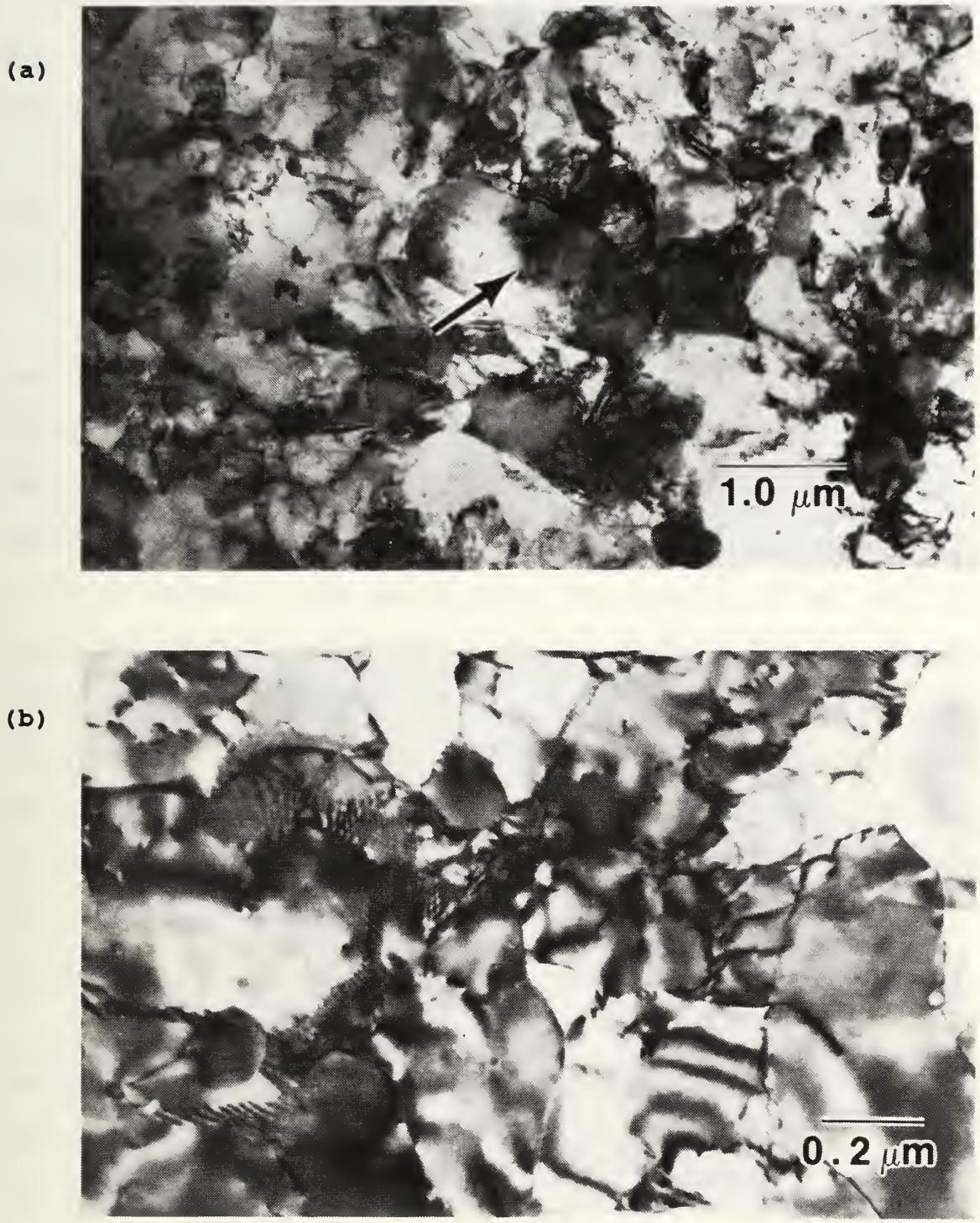

Figure 16. Representative bright field TEM micrographs of alloy 2090 as forged, aged, and rolled to a true strain of 2.5 at 300°C with 30 min reheating intervals between passes. Arrow indicates a T_2 precipitate in (a), and the typical substructure is shown in (b).

comparison with previous work with the Al-Mg-X series [Ref. 6]. Figure 17a provides a more detailed look at the morphology of the precipitate, with its blocky appearance and featureless internal structure. The precipitate is identified as T2 by its corresponding selected area diffraction (SAD) pattern of Figure 17b, showing the characteristic five-fold symmetry of T_2 [Ref. 20].

The second type of morphology present in the as-rolled material is represented in Figure 18. The notable feature of this microstructure is the precipitates aligning themselves in the rolling direction. SAD and bright field/ dark field (BF/DF) pairs (Figure 19) show these precipitates to be T_1 aligned on a (111) habit plane. It appears that T_1, which is known to exhibit (111) habit planes, has coalesced during rolling, becoming long thin plates of T_1 oriented on the (111) matrix planes, which are in turn parallel to the rolling direction. The discontinuous appearance of the precipitate, along with the fact that this morphology does not persist throughout the specimen, suggests that the precipitate may be in a transitional state, i.e., metastable.

The third type of microstructure present in the as-rolled material is shown in Figure 20a. Isolated areas of cracking were noticed throughout the sample, along with a distinctly rectangular shape to the precipitates, which also exhibited five-fold symmetry in their diffraction patterns (T_2), Figure 20b. The large size of the precipitate (3-4 μm by 1 μm)

(a)

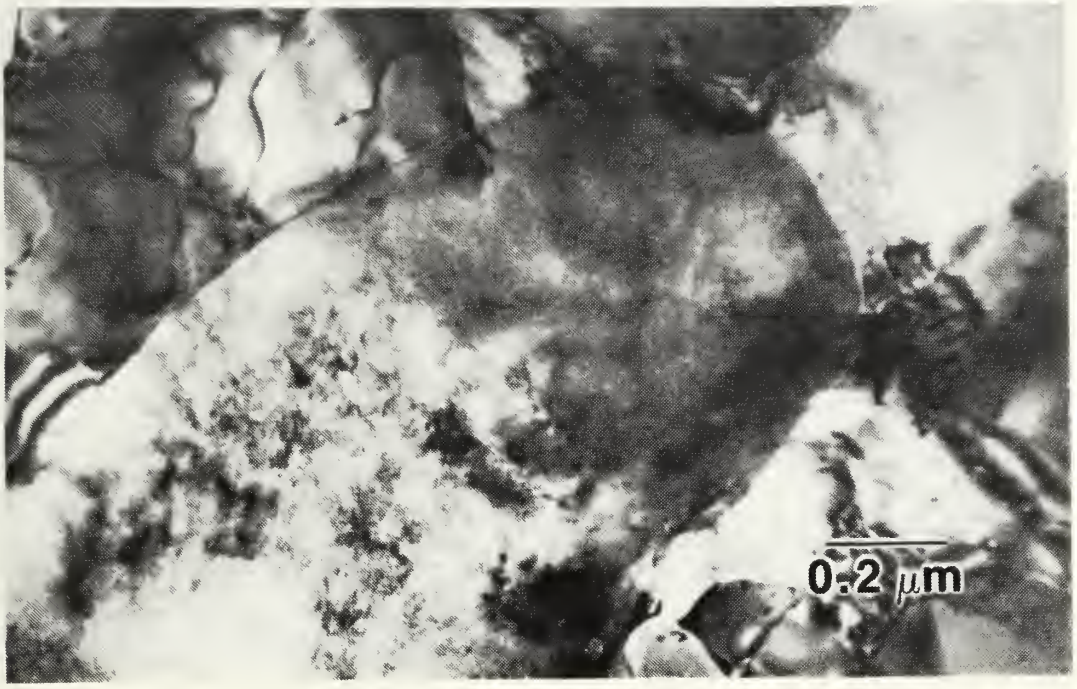

(b)

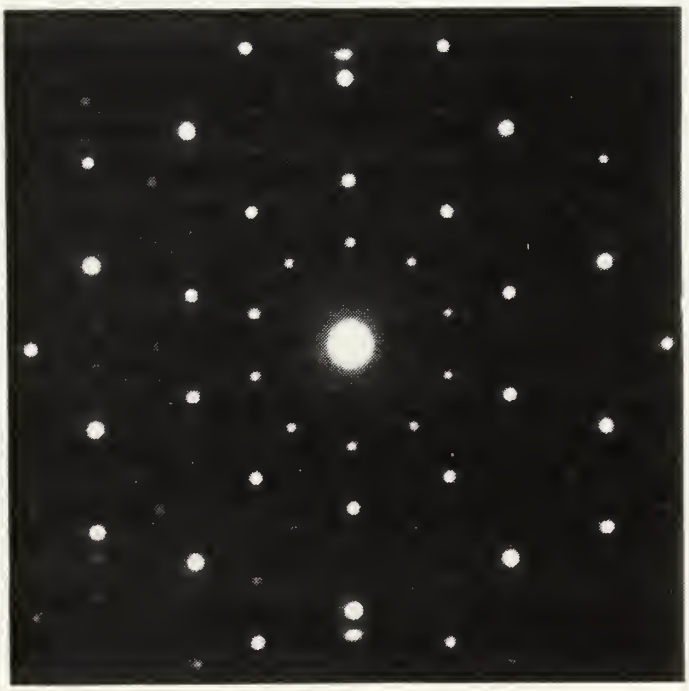

Figure 17. (a) Higher magnification TEM micrograph of particle identified in the previous figure. Note blocky morphology and large (1-2 μm) size. (b) Characteristic five-fold symmetry identifying the particle as T_2.

(a)

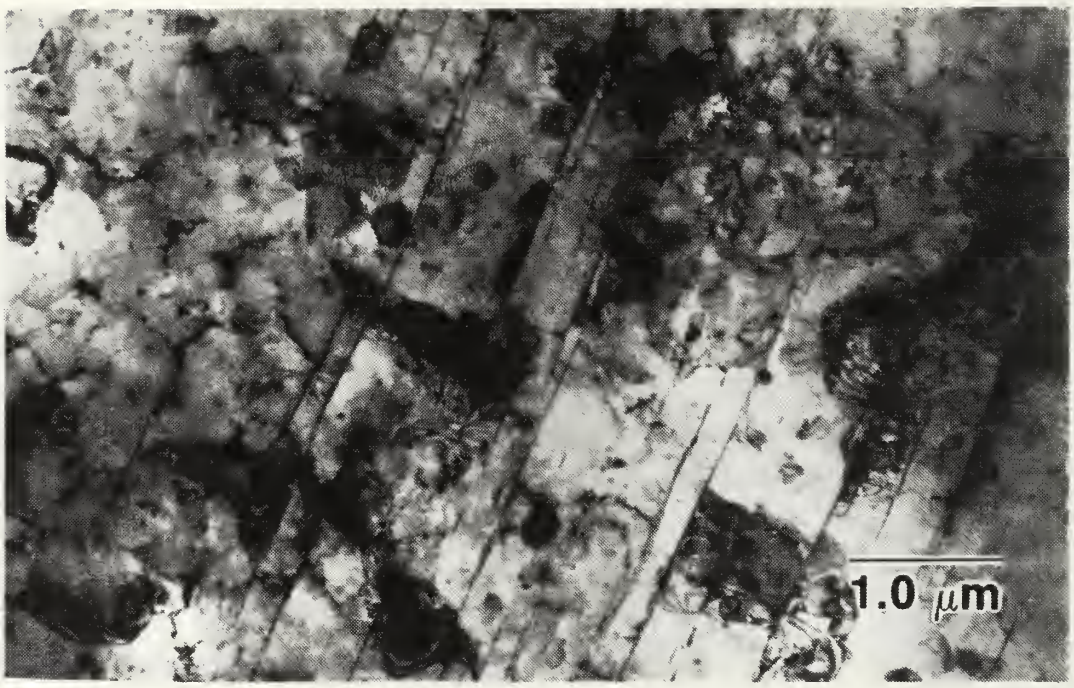

(b)

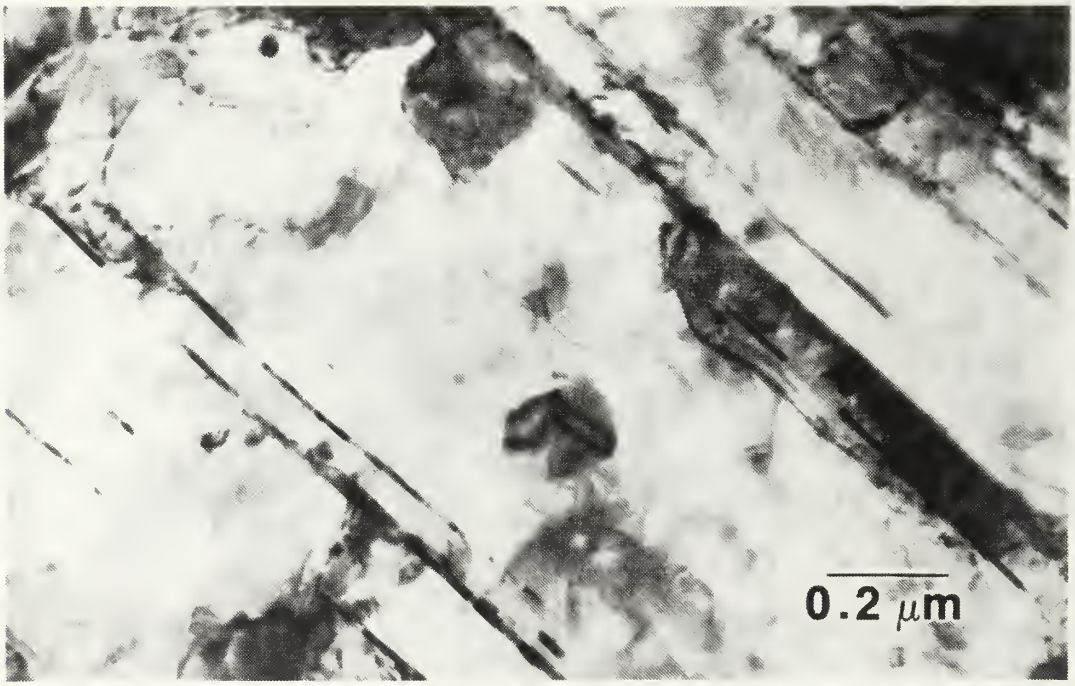

Figure 18. Second type of representative area found in material forged, aged and rolled at 300°C with 30 min reheat intervals between passes, (a). Note precipitates are aligned parallel to the rolling direction in (b).

(a)

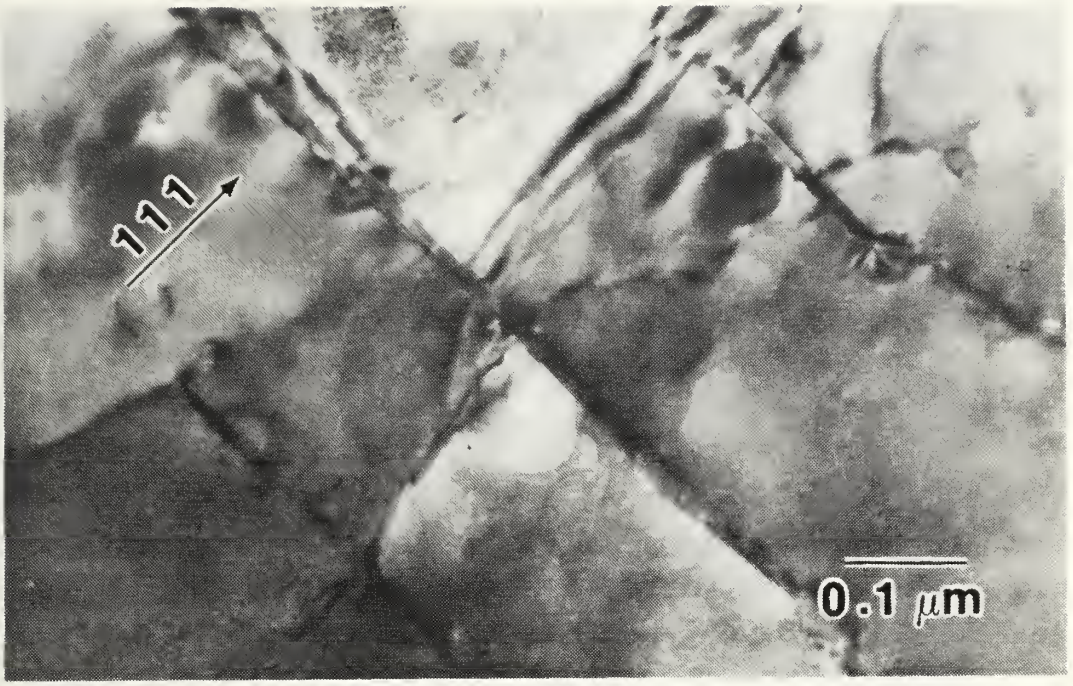

(b)

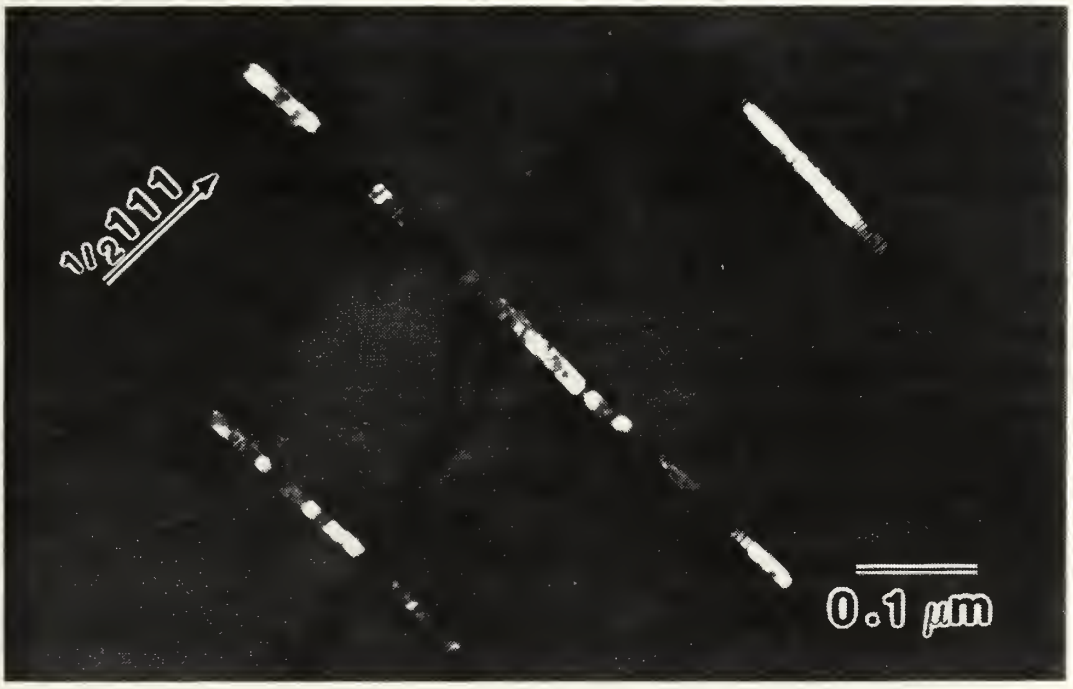

Figure 19. Bright field, (a) dark field, (b), pair of TEM micrographs from previous figure showing an example of T_1 precipitates residing on (111) habit planes.

(a)

(b)

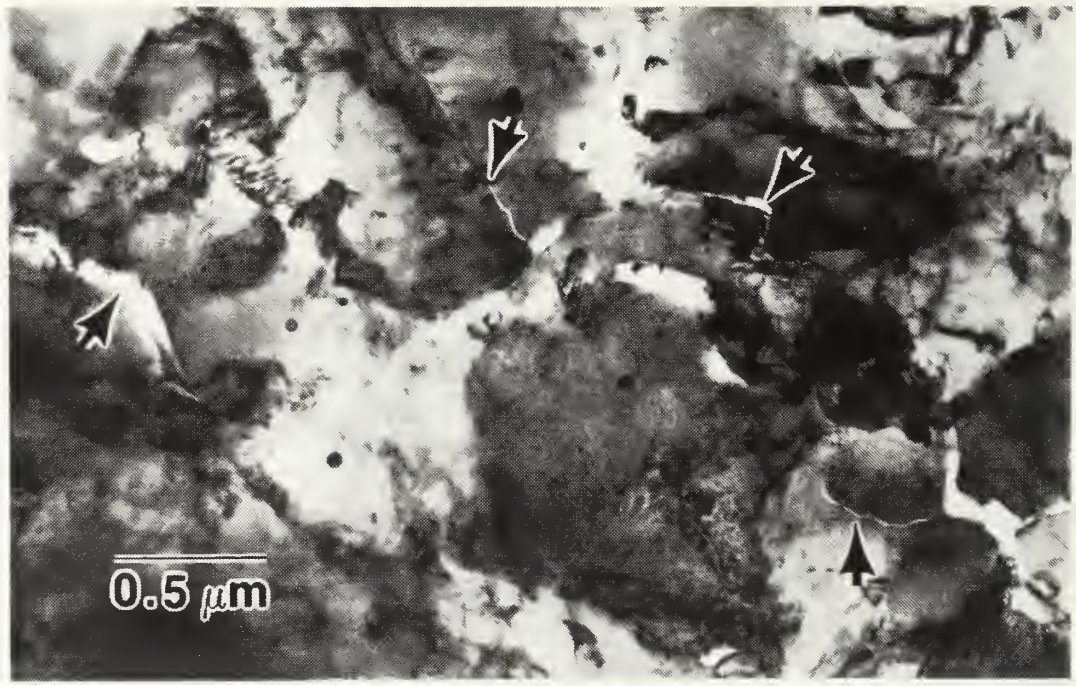

Figure 20. Areas of cracking found in alloy 2090 as forged, aged and rolled at 300°C with 30 min reheat intervals : (a) a fractured T_2 precipitate and (b) cracking associated with particle/matrix decohesion.

coupled with a fissure across the midpoint, might be expected to degrade mechnical properties. The cracks also suggest that the precipitates are brittle, and cracking is found in both large and small precipitates (Figure 20a).

The microstructure apparent at the conclusion of warm rolling includes a high dislocation density and both T_1 and T_2 phases. The aligned T_1, and the cracking of the T_2 would be expected to have an adverse effect on the resultant mechanical properties in the absence of any further evolution of the microstructure.

D. MICROSTRUCTURAL CONDITION AT THE ONSET OF TENSILE TESTS

The changes in microstructure upon heating the as-rolled material to a test temperature of 370°C are illustrated in Figure 21. TEM studies were conducted upon the grip section of the specimen exhibiting the largest ductility, when tensile tested at 370°C following warm rolling at 300°C with a 30 minute reheating interval between rolling passes. The grip section experiences no deformation during tensile testing, and hence represents the as-rolled material, heated to forming temperature, but without the effects of plastic deformation. Figure 21 reveals an even distribution of precipitates and (sub)grain size of 1-2μm . It should be noted that these TEM studies did not include a quantitative assessment of the boundaries to determine whether the observed microstructure consisted primarily of grains or subgrains.

(a)

(b)

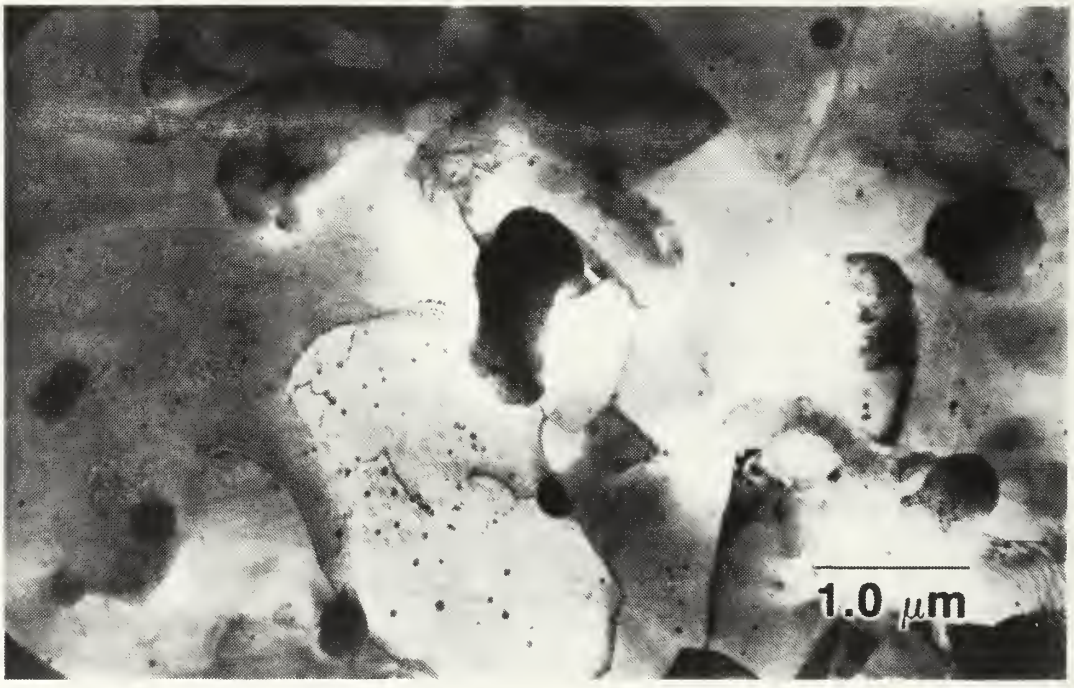

Figure 21. Bright field TEM micrographs, (a) and (b), of the grip section of alloy 2090. The microstructure is representative of the condition of the material at the onset of tensile testing at 370°C. Note the 1-2 μm particle size and the different morphologies.

Figure 22 indicates the second phase to be distributed in the size range from 0.5 μm to 1.5μm. Most of the precipitates were identified to be T_2 by the characteristic five-fold symmetry of their selected-area diffraction patterns. This suggests that the T_1 phase, noted within the grain interiors in the as forged material, may have transformed to T_2. Deformation of the structure developed by annealing alone might be expected accelerate the kinetic reactions such that the second phase present becomes predominantly T_2. The structure resulting from this TMP would be closer to equilibrium, as straining would tend to accelerate approach to the equilibrium state. This suggests that, for the composition of this particular alloy, the suggested phase boundary between the Al+T_1+T_2 three phase region and Al+T_2 two phase region should be somewhat to the left of that proposed by Hardy and Silcock and subsequently used by others.

As mentioned earlier, it was anticipated that the Zr addition to the alloy would be present as a dispersion of spheroidal $ZrAl_3$ precipitates. Figure 23a shows an example of such precipitates within the matrix of the material. The particles are coherent and vary from 20-50 nm in size. It is also apparent from this micrograph that they have some retarding influence on the migration of dislocations. However, as shown in Figure 23b, it is evident that the much larger T_2 precipitates interact more strongly with boundaries in the structure. The micrograph depicts a T_2 precipitate at

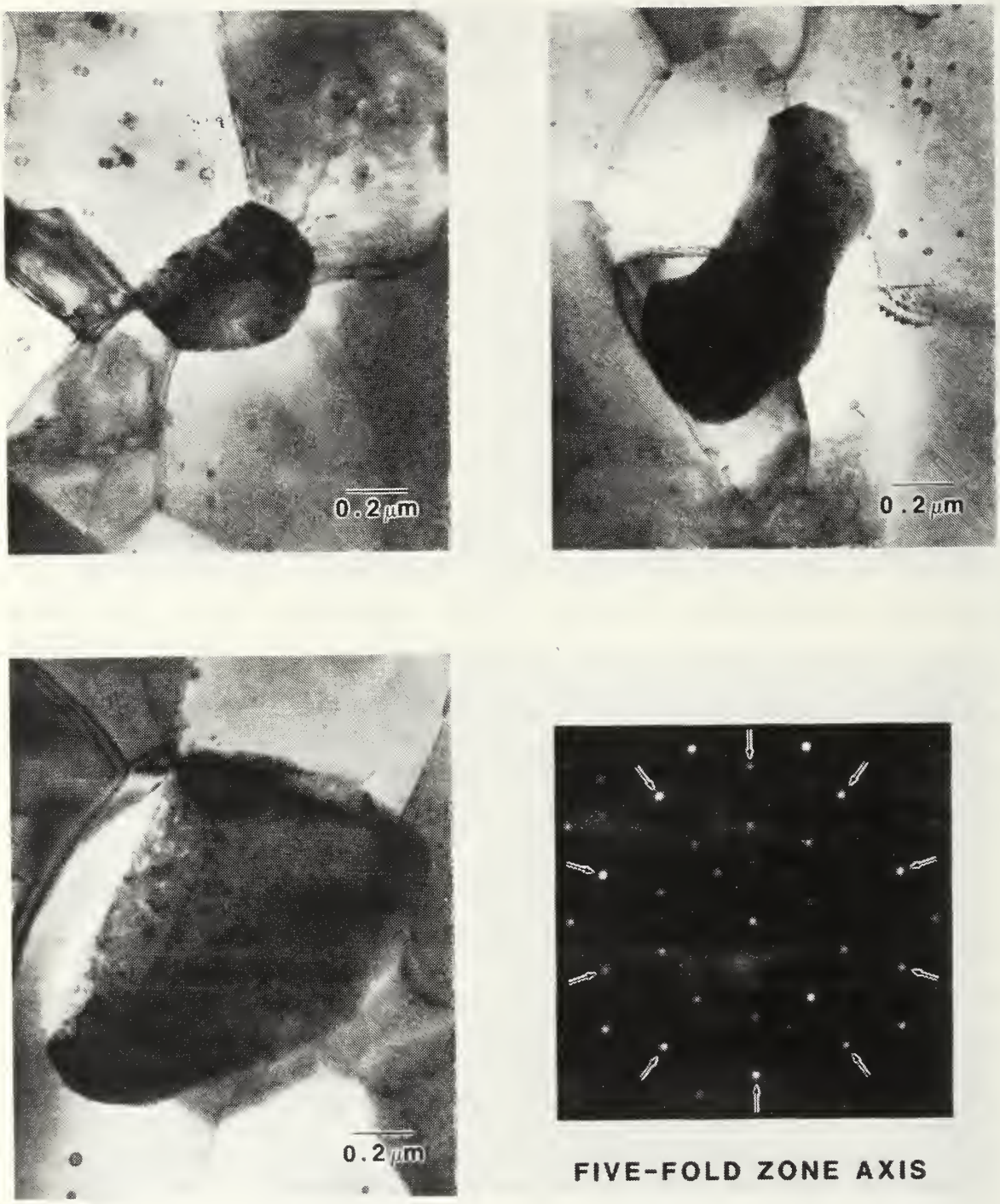

Figure 22. Relative size distribution of T_2 precipitates found in grip section of material at the onset of tensile testing at 370°C. Particle size ranges from 0.5 μm to 1.5 μm and all of the precipitates shown exhibit the five-fold symmetry, documented to be characteristic of T_2 [Ref. 20].

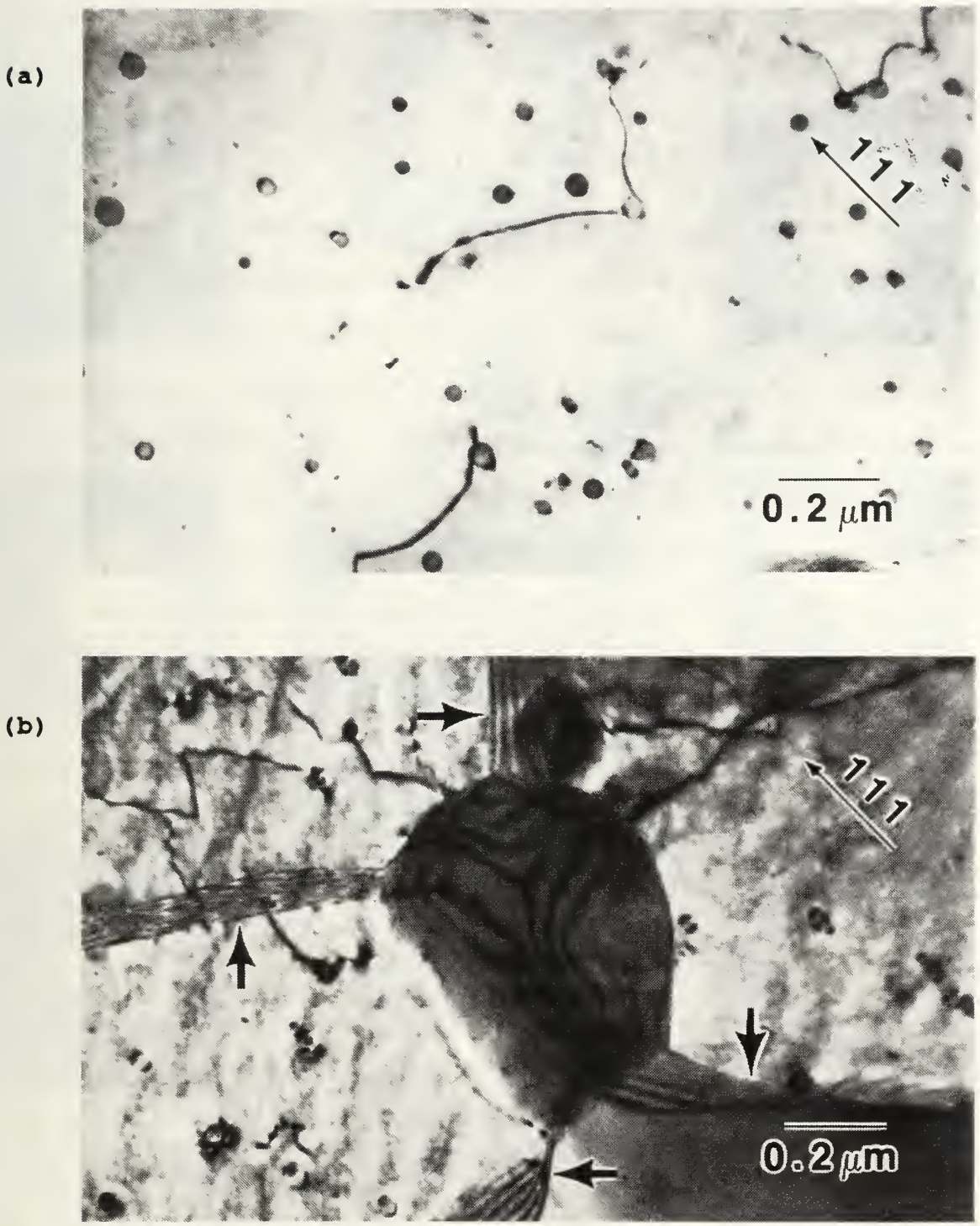

Figure 23. Bright field TEM micrographs of (a) $ZrAl_3$ particles precipitated coherently in the matrix, and (b) A T_2 precipitate residing on a boundary triple junction. Arrows indicate the boundaries adjacent to the precipitate.

a triple junction in the structure, with the associated boundaries indicated by the arrows. This indicates that T_2 may be performing a role similar to the β phase in the Al-Mg series.

The overall appearance of the microstructure presented thus far is very similar to that obtained in the Al-Mg-X system [Ref. 6]. Since a fine microstructure and uniform dispersion of second phase appear to have been achieved, the disappointing elongations achieved with this TMP must be as a result of failure to create the other key ingredient to superplastic response, high angle boundaries.

Figure 24 shows the same T_2 particle of Figure 23b, with corresponding SAD patterns from adjacent regions, indicating the various misorientations between adjacent (sub)grain boundaries. The patterns indicate predominately low angle ($\leq$ 5°) boundaries. Thus the desired high distribution of angle boundaries has not been achieved that would allow substantial grain boundary sliding to occur.

E. SUMMARY

In order to bring Al 2090 into service as quickly as possible, commercial sized ingots were produced before the physical metallurgy of the alloy was fully understood. This created a number of problems, particularly with respect to the precipitation sequence in the alloy at various temperatures. In fact, production was ceased at one point in

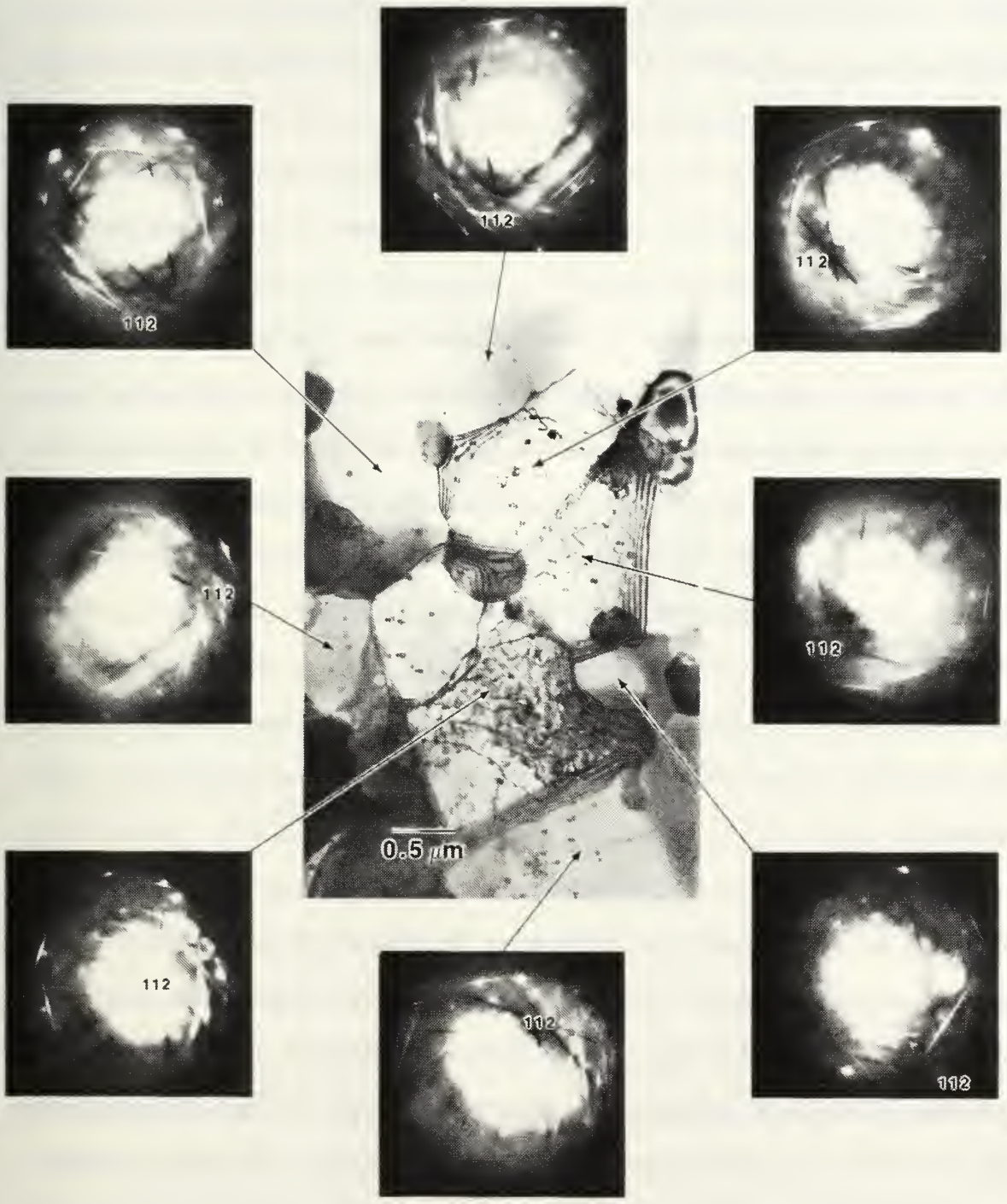

Figure 24. Bright field TEM micrograph and corresponding SAD patterns indicating the misorientation across various boundaries in the microstructure at the onset of tensile testing at 370°C. Analysis of the data indicates that the boundaries are predominantly low-angle in nature.

the development because the short transverse mechanical properties in plate fabricated above a certain thickness proved to be inconsistent and far below design expectations. This was attributed to solute segregation at grain boundaries and subsequent embrittlement as a result of intergranular second phase precipitation. Attempts to alleviate these problems centered on extensive homogenization treatments followed by stretch plus age treatments designed to eliminate long range segregation and reduce the degree of second phase precipitation on grain boundaries. The stretch took the form of cold working to strains of around 6% to introduce dislocation structures into the prior grain structure. The temperatures for subsequent aging were selected to promote the formation of the T_1 phase intragranularly and significant improvements in the isotropic mechanical properties were noted.

In the specific alloy of interest here, the homogenization treatment of annealing at 540°C for a period of only three hours in conjunction with forging at 480°C reflected the fact that the as-received material was already in a T8 condition. However, if the as-received material exhibited the anisotropic mechanical properties noted above, then it is probable that such a homogenization treatment may be insufficient. This was confirmed by the unsuccessful attempts to roll the material in the short transverse direction of the as-received sheet following the homogenization treatment designed for this

investigation. It is anticipated that further work on this batch of material will focus on extending the high temperature annealing times prior to intermediate temperature thermomechanical processing in order to ensure complete homogenization in the as-received microstructure.

The prior cold work, in the form of rolling to 10% strain at ambient temperature, was intended to promote intragranular precipitation. As a result of the controversy associated with the precipitation sequence at this temperature, and also regarding possible metastable phases and the morphology of the equilibrium phases, there was some uncertainty as to the nature of the second phase precipitates to be expected following this stage of the TMP. The data of Hardy and Silcock indicate that the aging and warm rolling temperatures lie in the $Al+T_1+T_2$ three phase region and these phases were observed. During the subsequent warm rolling, the relative ammounts of T_1 and T_2 change, with the T_2 content appearing to increase. The amount of T_1 precipitated as a coherent phase may thus reflect kinetic considerations. Also, the morphology of T_1 does not appear to change with deformation during the rolling, i.e., it is not "spheroidized" by the deformation. Rather, the T_1 appears to be substantially replaced by the T_2, although the mechanism for this was not determined.

In retrospect, this research indicates that there is little advantage to be gained from aging prior to warm rolling. In fact, intragranular precipitation of T_1 with its

inherent coherency and plate-like morphology may be detrimental when trying to promote the type of superplastic microstructures achieved in the Al-Mg alloys. Coherent T_1 particles may be cut by dislocations instead of stabilizing dislocation substructures. Also T_1 is observed to align with the rolling direction during warm rolling (Figure 18) and thus would result in an elongated rather than equiaxed grain structure, even if continuous recrystallization was observed. On the other hand, the development during rolling of the microstructure associated with the T_2 phase indicates that it has the correct morphology to facilitate development of an equiaxed structure. However, the microstructure obtained is not superplastic because the material still exhibits a fine **subgrain** structure as opposed to a fine **grain** structure. The mechanism of continuous recrystallization, alluded to in previous work, relies on the recovery of dislocations into boundaries thereby increasing misorientations. It is well documented that high-angle boundaries are necessary for a microstructure to support SPD mechanisms such as GBS. Thus, it is suggested that further studies eliminate the pre-aging step and in addition, increase the final rolling strain in an attempt to incorporate more dislocations into the constituent boundaries.

Bearing in mind the values for the T_1 and T_2 solvi, namely 520°C and 460°C respectively, it is interesting to speculate as to why maximum elongations were achieved at 370°C. As

temperature is increased above 370°C, the alloy moves closer to the T_1 side of the T_1+T_2 region of the phase diagram. This results in a lower volume fraction of T_2, thereby reducing the T_2 available to stabilize the microstructure during tensile testing. It may be noted that maximum elongations were achieved in the Al-Mg alloys at a temperature of 300°C, which corresponds to 0.9 of the β solvus temperature (365°C). Similarly in the Al 2090 alloy the best ductilities were obtained at 370°C which is also 0.9 of the solvus temperature for the T2 phase (460°C). This observation suggests again the roles of the T_2 in 2090 and β in the Al-Mg alloys to be similar.

V. CONCLUSIONS

A variety of techniques have been employed to determine the superplastic response of Al 2090 following thermomechanical processing at intermediate temperatures. The conclusions of the present study may be listed as follows:

1. Rolling at 300°C with 30 minute reheating intervals between passes produced better ductility over the material processed at 350°C using the same TMP schedule.

2. Processing the material such that the final rolling direction is parallel to the rolling direction of the original plate allowed for the best ductilities in subsequent tensile tests.

3. In comparison with previous thesis work done at NPS, aging at 350°C for 4 hours following initial forging and 10% cold working resulted in no significant improvement in ductility.

4. The highest ductilities of 215-245 pct. at a strain rate of 6.67×10^{-3} sec^{-1} were achieved during tensile testing at 370°C, below and above which ductility decreased.

5. TEM studies reveal refined structure following thermomechanical processing, but the boundaries are low angle in nature. This indicates that the material did not contain the high-angle boundaries necessary to support superplasticity.

VI. **RECOMMENDATIONS**

The following recommendations are made for further study:

1. Extend the solution treatment times in an attempt to more thoroughly homogenize the initial microstructure, which in this study has been shown to be somewhat anisotropic in nature.

2. Remove the forging, cold working and aging steps since the presence of the T_1 phase has proven to be detrimental to subsequent microstructural development.

3. Select a rolling scheme which will promote the formation of T_2 precipitates in the range of 0.5-1.0 μm intragranularly.

4. Increase the final rolling strain in an attempt to convert the fine subgrain structure, as produced in this study, into a fine grain structure by continuous recrystallization.

APPENDIX

TENSILE TEST DATA

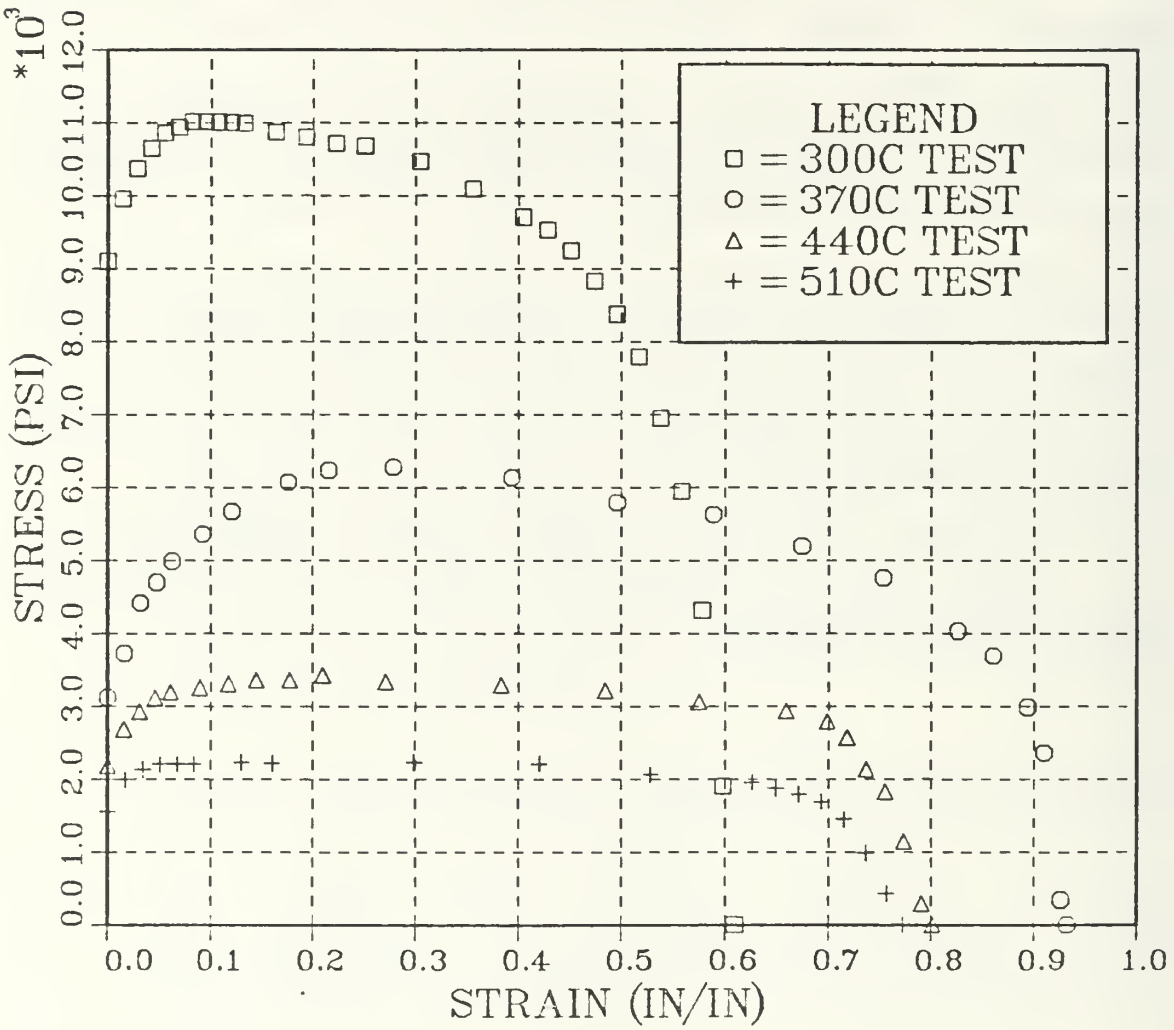

Figure A1. True Stress vs. True Strain as a function of test temperature at a strain rate of 6.67×10^{-3} sec^{-1}. The material was rolled at 300°C with 4 minute reheating intervals between rolling passes, in a direction parallel to the original plate long-transverse (LT) direction.

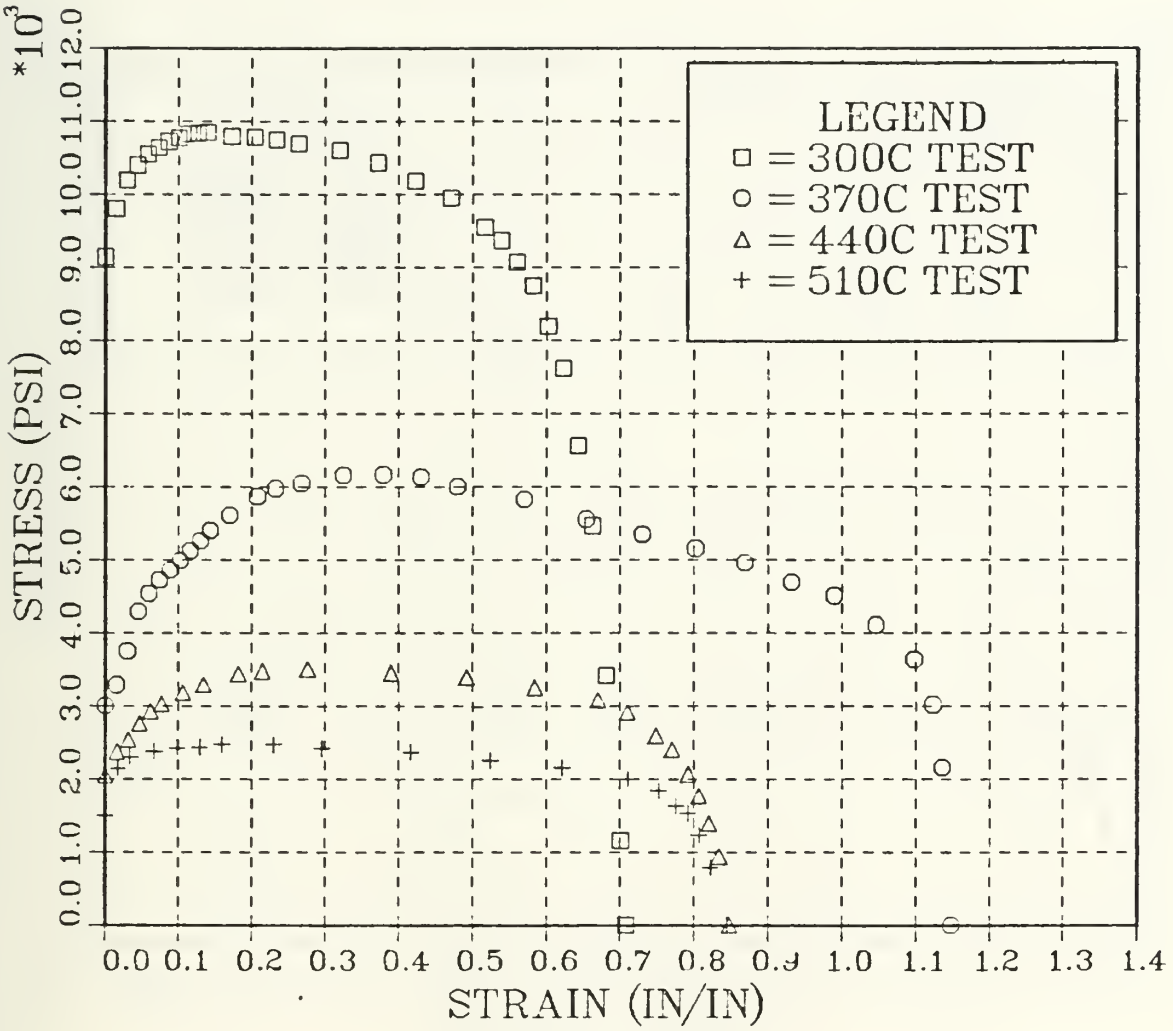

Figure A2. True Stress vs. True Strain as a function of test temperature at a strain rate of 6.67 x 10^{-3} sec^{-1}. The material was rolled at 300°C with 30 minute reheating intervals between rolling passes, in a direction parallel to the original plate long-transverse (LT) direction.

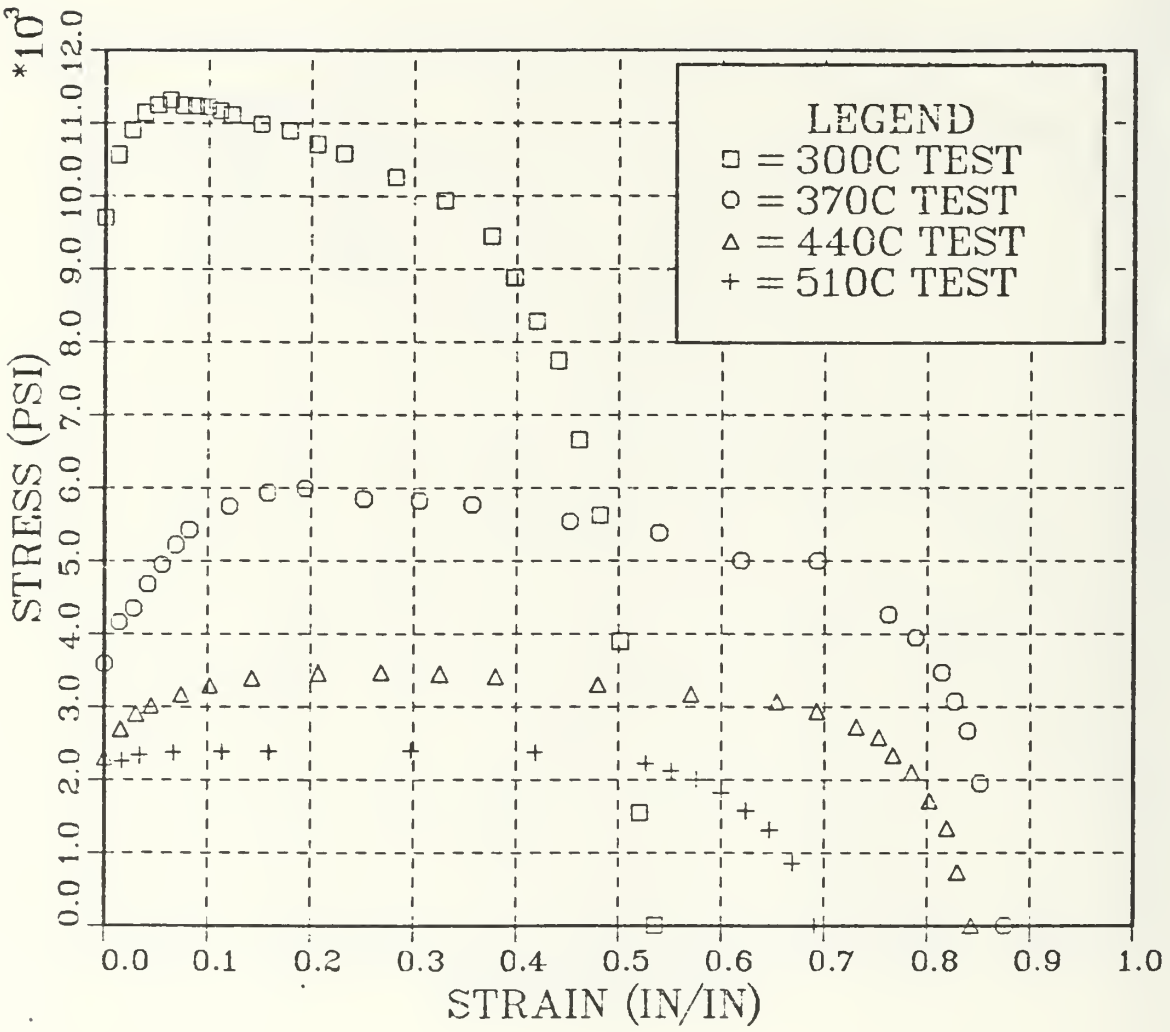

Figure A3. True Stress vs. True Strain as a function of test temperature at a strain rate of 6.67×10^{-3} sec^{-1}. The material was rolled at 350°C with 4 minute reheating intervals between rolling passes, in a direction parallel to the original plate long-transverse (LT) direction.

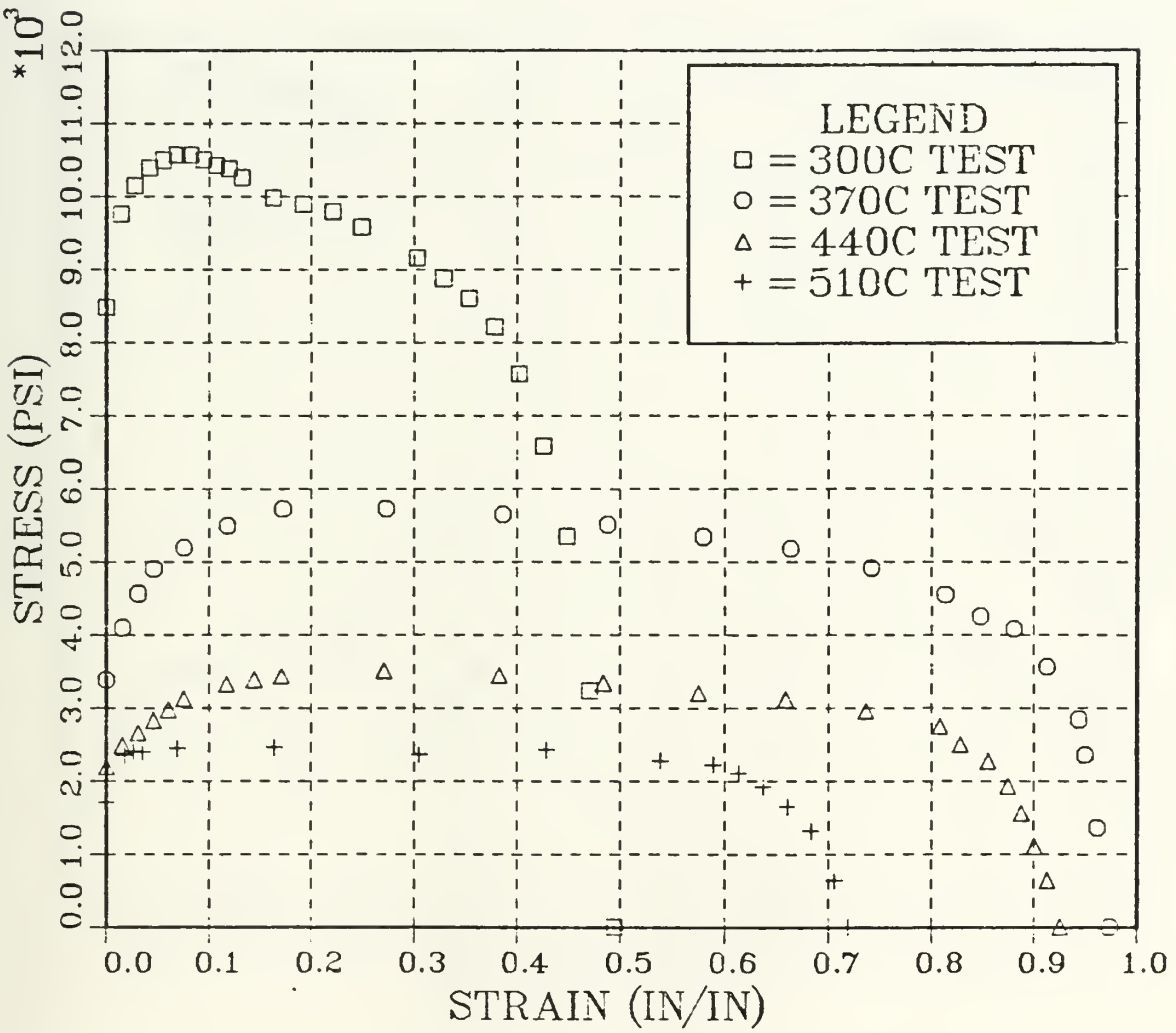

Figure A4. True Stress vs. True Strain as a function of test temperature at a strain rate of 6.67×10^{-3} sec^{-1}. The material was rolled at 350°C with 30 minute reheating intervals between rolling passes, in a direction parallel to the original plate long-transverse (LT) direction.

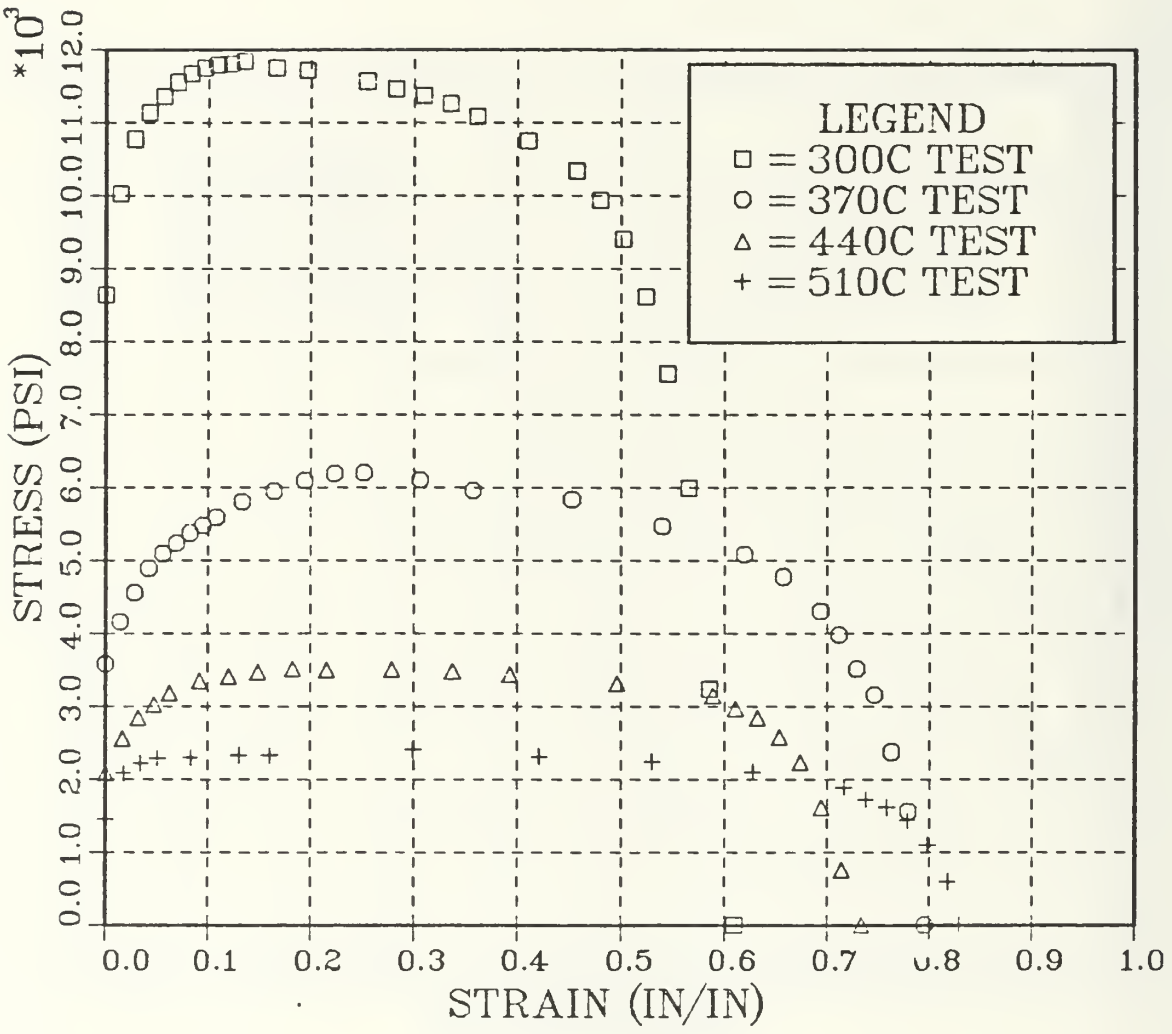

Figure A5. True Stress vs. True Strain as a function of test temperature at a strain rate of 6.67 x 10^{-3} sec^{-1}. The material was rolled at 300°C with 4 minute reheating intervals between rolling passes, in a direction parallel to the original plate longitudinal (L) direction.

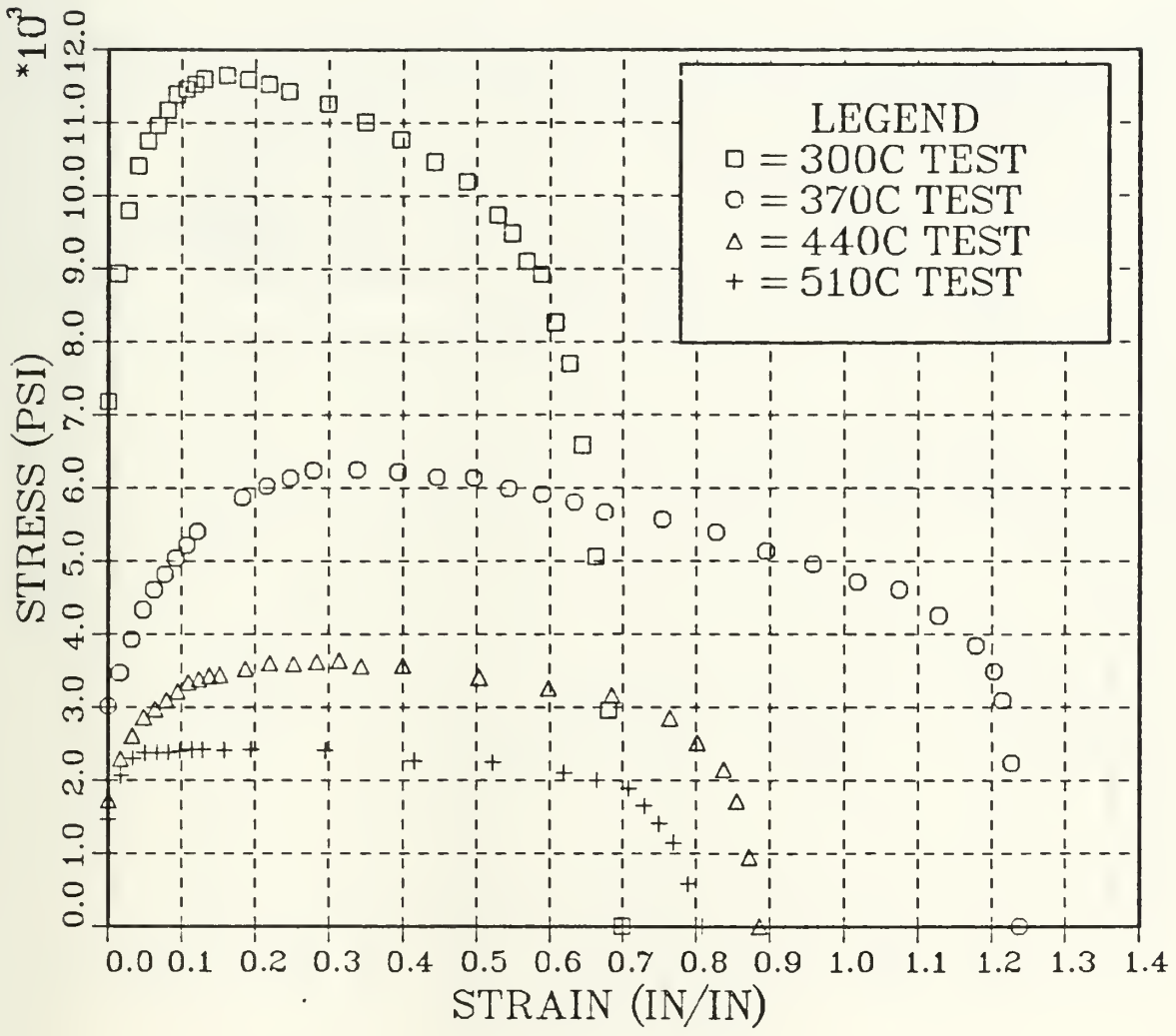

Figure A6. True Stress vs. True Strain as a function of test temperature at a strain rate of 6.67×10^{-3} sec^{-1}. The material was rolled at 300°C with 30 minute reheating intervals between rolling passes, in a direction parallel to the original plate longitudinal (L) direction.

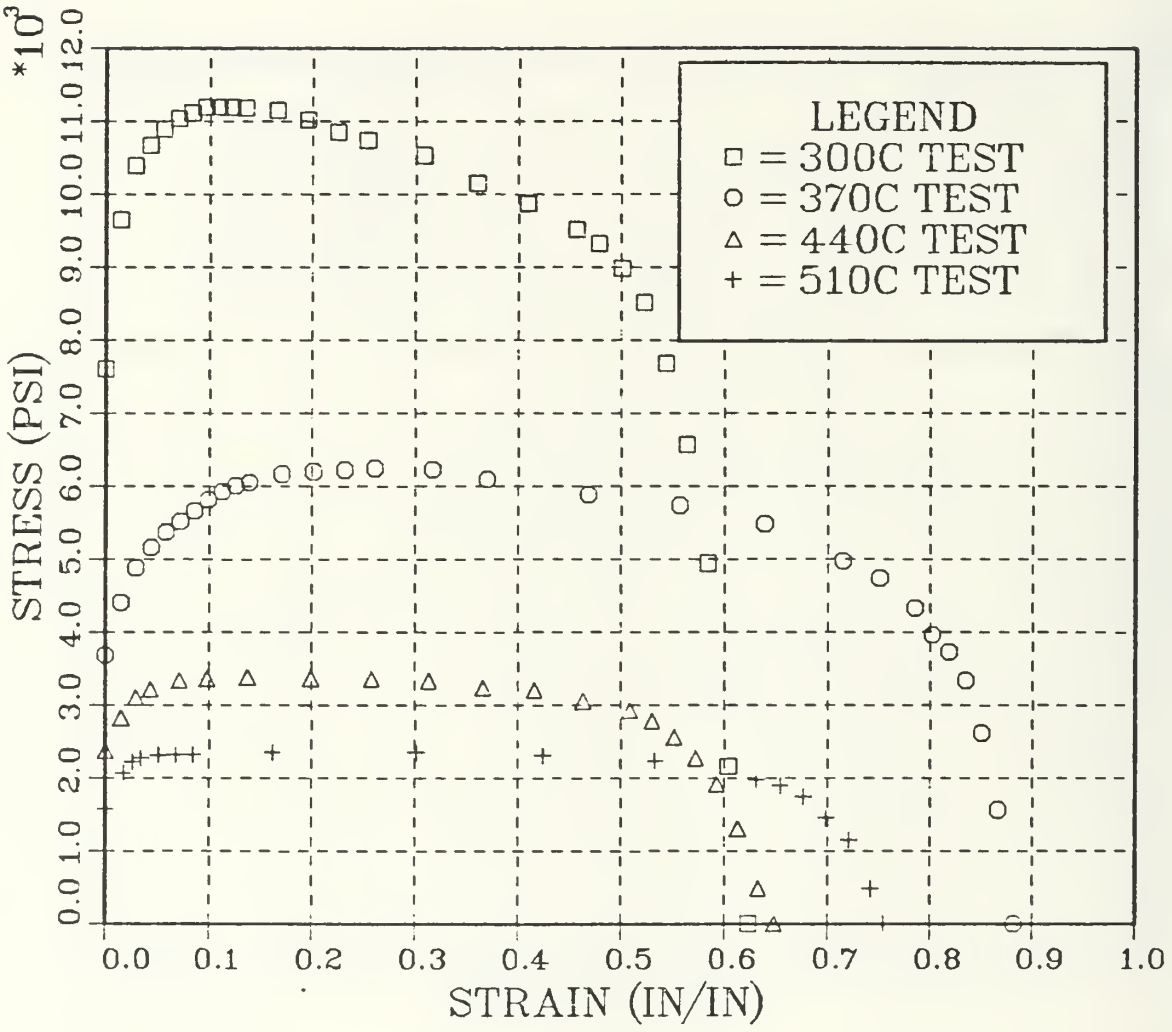

Figure A7. True Stress vs. True Strain as a function of test temperature at a strain rate of 6.67×10^{-3} sec^{-1}. The material was rolled at 350°C with 4 minute reheating intervals between rolling passes, in a direction parallel to the original plate longitudinal (L) direction.

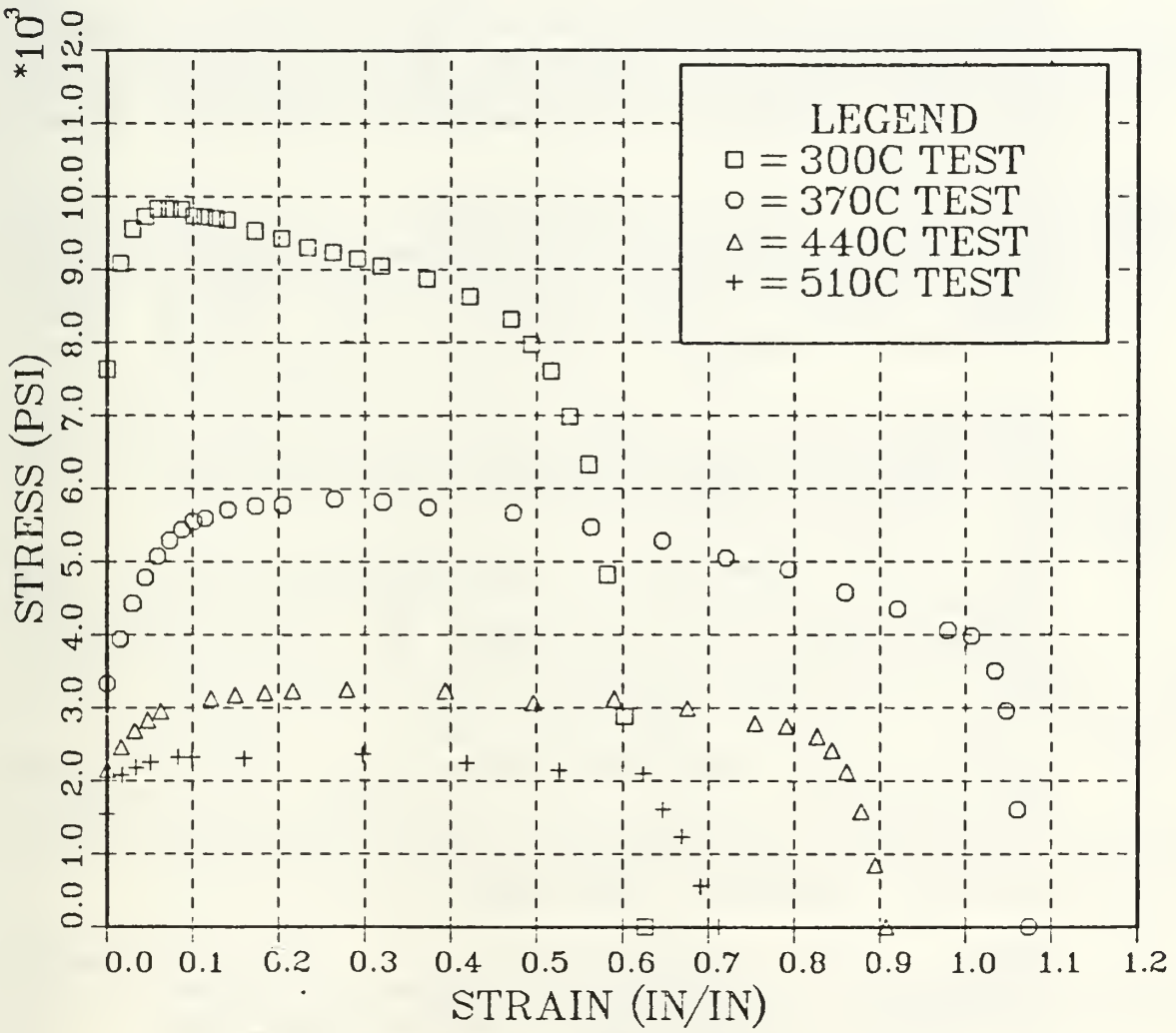

Figure A8. True Stress vs. True Strain as a function of test temperature at a strain rate of 6.67×10^{-3} sec^{-1}. The material was rolled at 350°C with 30 minute reheating intervals between rolling passes, in a direction parallel to the original plate longitudinal (L) direction.

LIST OF REFERENCES

1. Miller, W. S., White, J., and Lloyd, D. J., "The Metallurgy of Al-Li Based Alloys", Aluminum Alloys: Their Physical and Mechanical Properties, Vol. III, edited by Starke, E. A. Jr, and Sanders, T. H. Jr, pp. 1807-1809, Conference Proceedings, Chameleon Press, London, 1986.

2. Summerson, T. J., and Sprowls, D. O., "Corrosion Behavior of Aluminum Alloys, Aluminum Alloys: Their Physical and Mechanical Properties, Vol. III, edited by Starke, E. A. Jr, and Sanders, T. H. Jr, p. 1584, Conference Proceedings, Chameleon Press, London, 1986.

3. McNelley, T. R., Lee, E.-W., and Mills, M. E., "Superplasticity in a Thermomechanically Processed High Mg, Al-Mg Alloy", Metallurgical Transactions A, v. 17A, pp. 1035-1042, 1986.

4. Lee, E.-W., McNelley, T. R., Stengel, A. F., "The Influence of Thermomechanical Processing Variables on Superplasticity in a High Mg, Al-Mg Alloy", Metallurgical Transactions A, v. 17A, pp. 1043-1050, 1986.

5. Hales, S. J., and McNelley, T. R., "Fine-Grained Superplasticity at 300°C in a Wrought Al-Mg Alloy", Superplasticity in Aerospace, edited by Heikenen, H. C., and McNelley, T. R., pp. 61-76, Conference Proceedings, TMS-AIME, Warrendale, PA, 1988.

6. Hales, S. J., and McNelley, T. R., "Microstructural Evolution by Continuous Recrystallization in a Superplastic Al-Mg Alloy", Acta Metallurgica, v. 26, No.5, pp. 1229-1239, 1988

7. Glazer, J., Morris, J. W. Jr., "Thermomechanical processing of Two-Phase Al-Cu-Li-Zr Alloy", Aluminum-Lithium Alloys III, edited by Baker, C., and others, pp. 191-198, Conference Proceedings, Institute of Metals, London, 1985.

8. Ashton, R. F., and others, "Processing Al-Li-Cu-(Mg) Alloys", Aluminum-Lithium Alloys III, edited by Baker, C., and others, pp. 66-77, Conference Proceedings, Institute of Metals, London, 1985.

9. Rioja, R. J., and others,"Precipitation Reactions, Strength and Toughness of Al-Li-Cu Alloys, Aluminum Alloys: Their Physical and Mechanical Properties, Vol. III, edited by Starke, E. A. Jr., and Sanders, T. H. Jr., pp. 1781-1797, Conference Proceedings, Chameleon Press, London, 1986.

10. Cho, C. W., and others, "Superplasticity of 2090 SPF Sheet at Hot Rolled Gauge", 4th International Aluminum Lithium Conference, edited by Champier, G., and others, pp. 277-283, Les Editions de Physique, Paris, 1987.

11. Bretz, P. E. and Sawtell, R. R., "Alithalite Alloys: Progress, Products and Properties" , Aluminum-Lithium Alloys III, edited by Baker, C., and others, vol. III, pp. 47-49, Conference Proceedings, Institute of Metals, London, 1985.

12. Navy Times, p. 36, May 2, 1988.

13. Balmuth, E. S. and Schmidt, R., "A Perspective on the Development of Aluminum-Lithium Alloys", Aluminum-Lithium Alloys, edited by Sanders, T. H. Jr. and Starke, E. A., pp. 69-88, Conference Proceedings, TMS-AIME, Warrendale, PA, 1981.

14. Quist, W. E., Narayanan, G. H., and Wingert, A. L., "Aluminum-Lithium Alloys for Aircraft Structure - An Overview", Aluminum-Lithium Alloys II, edited by Sanders, T. H. Jr. and Starke, E. A. Jr., pp. 313-334, Conference Proceedings, TMS-AIME, Warrendale, PA, 1984.

15. Hardy, H. K. and Silcock, J. M., "The Phase Sections at 500°C and 350°C of Al-rich Al-Cu-Li Alloys", Journal of the Institute of Metals, v. 84, pp. 423-428, 1955/6.

16. Roeder, J. P., "Keynote Lecture to the Fourth Al-Li Conference", 4th International Aluminum Lithium Conference, edited by Champier, G., and others, pp. 1-7, Les Editions de Physique, Paris, 1987.

17. Bretz, P. E., "Alithalite Alloy Development and Production", 4th International Aluminum Lithium Conference, edited by Champier, G., and others, pp. 25-31, Les Editions de Physique, Paris, 1987.

18. Watson, T. J. and Bennetch, J. I., "The Effect of Microstructure on the SPF Behavior of Al-Li-X Alloys", Superplasticity in Aerospace, edited by Heikenen, H. C., and McNelley, T. R., pp. 261-297, Conference Proceedings, TMS-AIME, Warrendale, PA, 1988.

19. Huang, J. C. and Ardell, A. J.,"Crystal Structure and Stability of T_1 Precipitates in Aged Al-Li-Cu Alloys", Materials Science and Technology, v. 3, p. 188, March 1987.

20. Gayle, F. W., "The Icosahedral Al-Li-Cu Phase", 4th International Aluminum Lithium Conference, edited by Champier, G., and others, pp. 481-488, Les Editions de Physique, Paris, 1987.

21. Mondolfo, L. F., Aluminum Alloys: Structure and Properties, pp. 413-415, Butterworths, London, 1976.

22. Underwood, E. E., "A Review of Superplasticity and Related Phenomena", Journal of Metals, pp. 914-919, December 1962.

23. Alden, T. H., "Review Topics in Superplasticity", Treatise on Materials Science and Technology, v. 6, edited by Arsenault, R., J., p. 226, Academic Press, N.Y., 1975.

24. Sherby, O. D. and Wadsworth, J., "Development and Characterization of Fine-Grain Superplastic Materials", Deformation Processing and Structure, edited by Krauss, G., pp. 355-389, American Society for Metals, 1984.

25. Hazzledine, P. M., "The Mechanisms of Superplasticity", Deformation of Multi-Phase and Particle Containing Materials, edited by Bilde-Sorensen and others, pp. 27-40, Riso National Laboratory, Roskilde, Denmark, 1983.

26. Smallman, R. E., Modern Physical Metallurgy, 4th ed., p. 452, Butterworths, London, 1985.

27. Brandon, D. G., "The Structure of High Angle Boundaries", Acta Metallurgica, v. 14, pp. 1479-1484, November, 1966.

28. Hamilton, C. H., Bampton, C. C., and Paton, N. E., "Superplasticity in High Strength Aluminum Alloys", Superplastic Forming of Structural Alloys, edited by Paton, N. E. and Hamiliton, C. H., pp. 173-189, Conference Proceedings, TMS-AIME, Warrendale, PA, 1982.

29. Wert, J. A., "Grain Refinement and Grain Size Control", Superplastic Forming of Structural Alloys, edited by Paton, N. E. and Hamiliton, C. H., pp. 69-83, Conference Proceedings, TMS-AIME, Warrendale, PA, 1982.

30. B. M. Watts, and others, "Superplasticity in Al-Cu-Zr Alloys Part II: Microstructural Study", Metal Science Journal, v. 6, p. 189-198, June 1976.

31. Ricks, R. A. and Winkler, P. J., "Superplastic Optimization for Diffusion Bonding Applications in Al-Li Alloys", Superplasticity and Superplastic Forming, edited by Hamilton, C. H., and others, in press, Conference Proceedings, TMS-AIME, Warrendale, PA, 1988.

32. Spiropoulos, P. T., Thermomechanical Processing of Al Alloy 2090 for Grain Refinement and Superplasticity, M.S. Thesis, Naval Postgraduate School, Monterey, California, December 1987.

33. Regis, H. C., Processing of 2090 Aluminum Alloy for Superplasticity, M.S. Thesis, Naval Postgraduate School, Monterey, California, June 1988.

34. Annual Book of ASTM Standards, v. 02.02, pp. 1044-1055, American Society for Testing and Materials, 1986.

35. Lee, E.-W. and McNelley, T. R. "Microstructure Evolution during Processing and Superplastic Flow in a High Magnesium Al-Mg Alloy", Materials Science and Engineering, v. 93, p. 45-55, 1987.

36. Metals Handbook, 9th ed., v. 9, p. 354, American Society for Metals, 1986.

INITIAL DISTRIBUTION LIST

		No. Copies
1.	Defense Technical Information Center Cameron Station Alexandria, VA 22304-6145	2
2.	Library, Code 0142 Naval Postgraduate School Monterey, CA 93943-5002	2
3.	Department Chairman, Code 69Hy Department of Mechanical Engineering Naval Postgraduate School Monterey, CA 93943-5000	1
4.	Professor T. R. McNelley, Code 69Mc Department of Mechanical Engineering Navl Postgraduate School Monterey, CA 93943-5000	5
5.	Dr. S. J. Hales, Code 69He Department of Mechanical Engineering Naval Postgraduate School Monterey, CA 93943-5000	1
6.	Naval Air Systems Command, Code AIR 931 Naval Air Sytems Command Headquarters Washington, DC 20361	1
7.	Dr. Eui-Whee Lee, Code 6063 Naval Air Development Center Warminster, PA 18974	1
8.	LCDR Gary E. Groh 850 Hillside Rd Naperville, IL 60540	2
9.	Dr. J. M. B. Losz, Code 69Lo Department of Mechanical Engineering Naval Postgraduate School Monterey, CA 93943-5000	1

Thesis
G8521 Groh
c.1 Processing of Aluminum alloy 2090 for superplasticity.